VOLUME 21, NUMBER 4, 2011

# Hippocampus

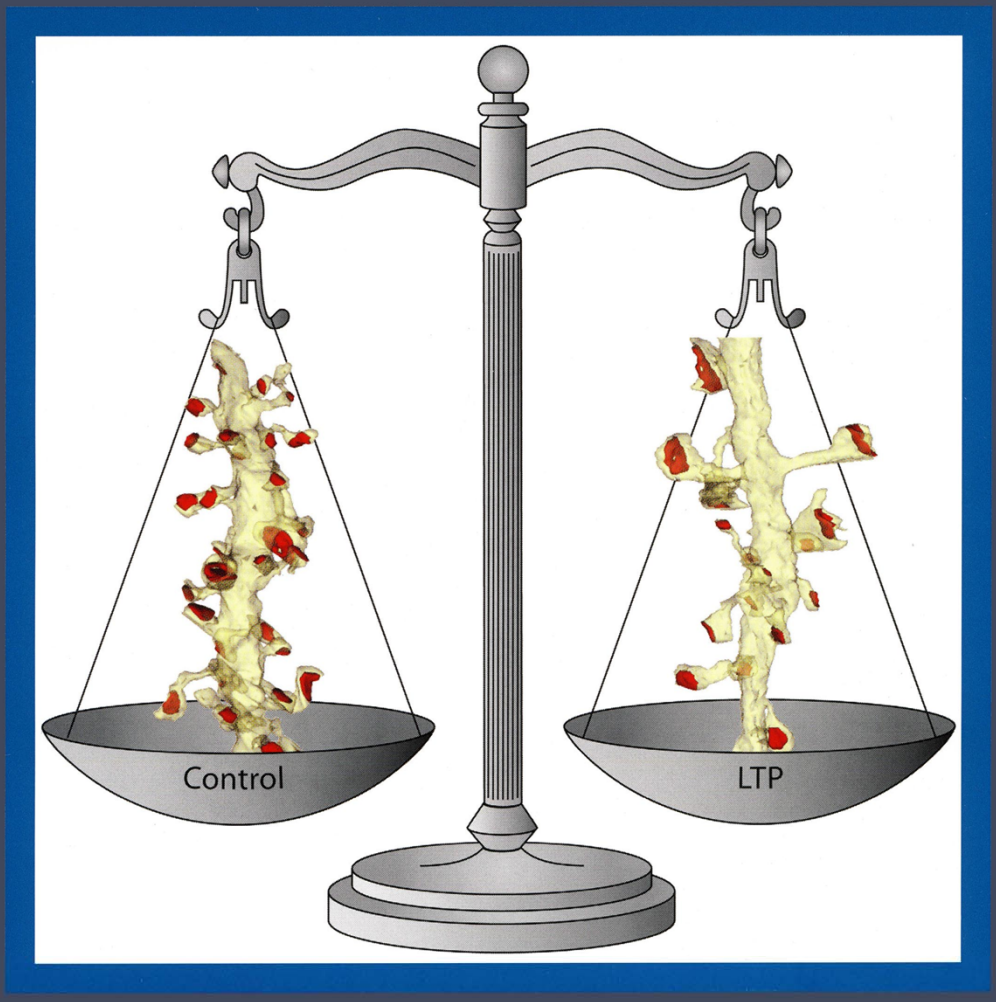


Coordination of size and number of excitatory and inhibitory synapses results in a balanced structural plasticity along mature hippocampal CA1 dendrites during LTP

Jennifer N. Bourne and Kristen M. Harris

WILEY-BLACKWELL
ISSN 1050-9631

*HIPPOCAMPUS 21:354–373 (2011)*

# Coordination of Size and Number of Excitatory and Inhibitory Synapses Results in a Balanced Structural Plasticity Along Mature Hippocampal CA1 Dendrites During LTP

Jennifer N. Bourne and Kristen M. Harris*

**ABSTRACT: Enlargement of dendritic spines and synapses correlates with enhanced synaptic strength during long-term potentiation (LTP), especially in immature hippocampal neurons. Less clear is the nature of this structural synaptic plasticity on mature hippocampal neurons, and nothing is known about the structural plasticity of inhibitory synapses during LTP. Here the timing and extent of structural synaptic plasticity and changes in local protein synthesis evidenced by polyribosomes were systematically evaluated at both excitatory and inhibitory synapses on CA1 dendrites from mature rats following induction of LTP with theta-burst stimulation (TBS). Recent work suggests dendritic segments can act as functional units of plasticity. To test whether structural synaptic plasticity is similarly coordinated, we reconstructed from serial section transmission electron microscopy all of the spines and synapses along representative dendritic segments receiving control stimulation or TBS-LTP. At 5 min after TBS, polyribosomes were elevated in large spines suggesting an initial burst of local protein synthesis, and by 2 h only those spines with further enlarged synapses contained polyribosomes. Rapid induction of synaptogenesis was evidenced by an elevation in asymmetric shaft synapses and stubby spines at 5 min and more nonsynaptic filopodia at 30 min. By 2 h, the smallest synaptic spines were markedly reduced in number. This synapse loss was perfectly counterbalanced by enlargement of the remaining excitatory synapses such that the summed synaptic surface area per length of dendritic segment was constant across time and conditions. Remarkably, the inhibitory synapses showed a parallel synaptic plasticity, also demonstrating a decrease in number perfectly counterbalanced by an increase in synaptic surface area. Thus, TBS-LTP triggered spinogenesis followed by loss of small excitatory and inhibitory synapses and a subsequent enlargement of the remaining synapses by 2 h. These data suggest that dendritic segments coordinate structural plasticity across multiple synapses and maintain a homeostatic balance of excitatory and inhibitory inputs through local protein-synthesis and selective capture or redistribution of dendritic resources.** © **2010 Wiley-Liss, Inc.**

**KEY WORDS: serial section transmission electron microscopy; 3D reconstruction; dendritic spine; polyribosomes; hippocampal slice; adult; ultrastructure**

**Center for Learning and Memory, Section of Neurobiology, Institute for Neuroscience, University of Texas, Austin, Texas**

Additional Supporting Information may be found in the online version of this article.

Grant sponsor: NIH; Grant numbers: NS21184, NS33574, EB002170.

*Correspondence to: Kristen M. Harris, Ph.D., Center for Learning and Memory, 1 University Station C7000, University of Texas, Austin, TX 78712. E-mail: kharris@mail.clm.utexas.edu

Accepted for publication 30 November 2009
DOI 10.1002/hipo.20768
Published online 25 January 2010 in Wiley Online Library (wileyonlinelibrary.com).

## INTRODUCTION

Structural synaptic plasticity is thought to be an essential feature of long-term potentiation (LTP), a cellular mechanism of learning and memory (Bliss and Collingridge, 1993; Yuste and Bonhoeffer, 2001; Bourne and Harris, 2008). Tetanic stimulation consisting of multiple trains of pulses delivered at 100 Hz for 1 s has often been utilized to elicit "saturating" LTP. Early electron microscopy (EM) studies in mature dentate gyrus showed evidence for altered synapse number and morphology within an hour after tetanic stimulation of the perforant pathway (Fifkova and Van Harreveld, 1977; Fifkova and Anderson, 1981; Desmond and Levy, 1983, 1986a,b; Trommald et al., 1990, 1996; Geinisman et al., 1991, 1993), with some spines and synapses remaining enlarged for several hours (Fifkova and Van Harreveld, 1977; Popov et al., 2004). However, delivery of tetanic stimulation elicited minimal changes in spine density or size in area CA1 of the mature hippocampus (Lee et al., 1980; Chang and Greenough, 1984; Sorra and Harris, 1998; Lang et al., 2004).

Recent work suggests that theta-burst stimulation (TBS) better resembles the endogenous neuronal firing patterns in the hippocampus (Morgan and Teyler, 2001; Buzsaki, 2002; Hyman et al., 2003), and can be more effective at producing LTP (Staubli and Lynch, 1987; Abraham and Huggett, 1997; Nguyen and Kandel, 1997; Raymond and Redman, 2002, 2006). Back-propagating action potentials are an important component of associative synaptic plasticity (Magee and Johnston, 1997, 2005) and multiple trains of TBS trigger postsynaptic action potentials that are necessary and sufficient to coordinate the intracellular signaling needed to sustain enduring LTP (Raymond, 2008). In contrast, tetanic stimulation results in a sustained depolarization of tetanized dendrites that prevents action potential back-propagation and reduces the amplitude and effectiveness of synaptic inputs on the tetanized dendrite (Whittington et al., 1997; Bracci et al., 1999; Vreugdenhil et al., 2005). TBS also elevates intracellular calcium from multiple sources and releases BDNF; events not elicited with tetanic stimulation (Larson et al., 1986; Abraham and Huggett, 1997; Kang et al., 1997;

Raymond and Redman, 2002, 2006). Thus, a systematic study of structural plasticity following TBS should more closely mimic the circumstances of LTP induction under conditions of learning.

Studies on structural plasticity have mostly targeted individual spines and synapses (Lang et al., 2004; Matsuzaki et al., 2004; Kopec et al., 2006, 2007; Tanaka et al., 2008; Corera et al., 2009; Lee et al., 2009). However, recent neural models predict that a nonlinear summation of synapses along a dendritic branch would markedly increase storage capacity (Poirazi and Mel, 2001; Polsky et al., 2004; Magee and Johnston, 2005). If so, then multiple dendritic spines along a single dendritic segment might function together as a computational unit. Physiological recordings and functional imaging supports this hypothesis (Gray et al., 2006; Losonczy and Magee, 2006; Tsuriel et al., 2006; Harvey and Svoboda, 2007; De Roo et al., 2008; Harvey et al., 2008; Losonczy et al., 2008; Rose et al., 2009; Zhong et al., 2009). Further support comes from investigations of the intracellular composition of hippocampal dendrites. For example, polyribosomes occur every 1–2 μm along the lengths of both immature and mature hippocampal dendrites and thus intersperse among 4–10 dendritic spines (Ostroff et al., 2002; Bourne et al., 2007b). Recycling and endosomal organelles that are critical for synaptic function occur at a lower frequency than one per spine, and thus might serve to coordinate structural plasticity along dendritic segments of about 10 μm in length (Spacek and Harris, 1997; Cooney et al., 2002; Park et al., 2006). Inhibitory synapses occur on average only once every 5–10 μm along the shaft of CA1 dendrites (Megias et al., 2001) and therefore could modulate synaptic function among many dendritic spines. Thus, analysis of whole dendritic segments could reveal a coordinated structural change among several synapses along a segment of dendrite during LTP.

To capitalize on this new understanding of coordinated synaptic plasticity, an important consideration is the number of synapses that actually undergo potentiation following induction of LTP. At one extreme, chemical LTP has been used to maximally stimulate all of the synapses in a slice (Hosokawa et al., 1995; Otmakhov et al., 2004; Kopec et al., 2006, 2007). At the other extreme, experiments have aimed to understand whether an individual dendritic spine can undergo structural plasticity in response to localized chemical induction (Engert and Bonhoeffer, 1999), glutamate uncaging (Matsuzaki et al., 2004; Tanaka et al., 2008), or minimal stimulation (Lang et al., 2004). Somewhere between these extremes lies the probable pattern exhibited during normal activation with learning (Buzsaki et al., 1987; Buzsaki, 2002). We have developed a paradigm using a concentric bipolar electrode that can be adjusted to activate most, if not all, of the axons passing beneath it, yet limit induction of LTP to a circumscribed region (Ouyang et al., 1997; Sorra and Harris, 1998; Ostroff et al., 2002; Bourne et al., 2007b). In this way, segments of dendrites in the path of TBS stimulation can be compared to those receiving only control stimulation outside the domain of TBS-LTP.

Analysis of dendritic segments should also reveal whether synaptogenesis occurs during LTP in the mature hippocampus. Live-imaging in young or cultured hippocampal neurons has demonstrated rapid spine turnover during LTP (Engert and Bonhoeffer, 1999; Maletic-Savatic et al., 1999; Nagerl et al., 2004, 2007; De Roo et al., 2008), but live imaging in the mature hippocampus has been more limited and revealed modest changes in spine dimensions (Hosokawa et al., 1995; Lang et al., 2004). Serial section transmission electron microscopy (ssTEM) has revealed indicators of synaptogenesis such as filopodia, stubby spines, and shaft synapses in mature hippocampus following ice-cold slice preparation (Kirov et al., 1999, 2004b) and synaptic inactivation (Petrak et al., 2005). Little is known, however, about whether synaptogenesis occurs on mature dendrites following the induction of LTP. Previous EM studies in mature hippocampal area CA1 found no changes in spine synapse size or number 1–2 h following tetanic or chemical stimulation (Sorra and Harris, 1998; Stewart et al., 2005), suggesting that if synaptogenesis occurs, it must be balanced by elimination. Therefore, analysis of dendritic segments at multiple time points is needed to learn more about the sequence of structural plasticity and whether synaptogenesis and elimination accompany LTP in the mature hippocampus.

Here we set out to understand structural synaptic plasticity in mature CA1 neurons in response to TBS-LTP using slices that were optimized for outstanding preservation of structure. We discovered evidence for rapid synaptogenesis following induction of TBS-LTP in the mature system. We learned that polyribosomes are even more responsive to structural plasticity following the more realistic TBS-LTP than following tetanic stimulation. We discovered a nearly perfect coordination of changes in synapse number and size for both excitatory and inhibitory synapses. Thus, the mature dendrites have a remarkable capacity for structural synaptic plasticity, rivaling that which occurs in the developing system.

## MATERIALS AND METHODS

### Preparation and Recording From Acute Hippocampal Slices

Hippocampal slices 400-μm thick were prepared from eight young adult male Long Evans rats aged 51–65 days old (weighing 219–361 g). Animals were anesthetized with halothane, decapitated, and slices were rapidly chopped using a Stoelting tissue chopper at room temperature (~25°C) using artificial cerebrospinal fluid (ACSF) containing (in mM): 116.4 NaCl, 5.4 KCl, 3.2 $CaCl_2$, 1.6 $MgSO_4$, 26.2 $NaHCO_3$, 1.0 $NaH_2PO_4$, and 10 D-glucose. Then slices were transferred immediately to nets positioned over wells containing ACSF at the interface of humidified $O_2$ (95%) and $CO_2$ (5%) and were maintained at 32°C for an average of 3 h (range: 2.25–3.5 h) in vitro before the onset of the recordings. Total time from decapitation to placing slices on the nets ranged from 5 min

and 21 s to 6 min and 33 s. Two concentric bipolar stimulating electrodes (100 μm outside diameter, Fred Haer, Brunswick, ME) were located 300–400 μm on either side of a single extracellular recording electrode placed in the middle of stratum radiatum (glass micropipette filled with 120 mM NaCl, Fig. 1A, arrow) for a total separation of 600–800 μm. We previously demonstrated that a distance of 400 μm between stimulating electrodes was sufficient to stimulate independent populations of inputs to CA1 pyramidal neurons (Sorra and Harris, 1998; Ostroff et al., 2002).

Extracellular field potentials were recorded using IGOR software (WaveMetrics, Lake Oswego, OR). The slope (mV per ms) of the field excitatory postsynaptic potential (fEPSP) was measured for 400 μs along the steepest segment of the negative field potential beginning 170–250 μs after the stimulus artifact and measured at the same position before and after LTP induction. An input–output (I/O) curve determined the range of responsiveness of the slices and the stimulus intensity was set just below population spike threshold and held constant throughout the remainder of the experiment. Stimulations were alternated between the control and TBS-LTP electrode once every 2 min at a 30-s interval between electrodes.

## TBS-LTP Paradigm

One slice was used per animal. A stable baseline was established for 30 min and then theta burst stimulation (TBS) (8 trains of 10 bursts at 5 Hz of 4 pulses at 100 Hz delivered 30 s apart (requiring 3.5 min in total)) was delivered to one stimulating electrode while the control electrode received no stimulation. The positions of the control and TBS-LTP electrodes were alternated between the CA3 and subicular side of the recording electrode counterbalancing across experiments. Responses from the control and TBS stimulating electrodes were monitored for 5 min, 30 min, or 2 h after the first train of TBS (i.e., 1.5 min, 26.5 min, or 1 h 56.5 min after the last train of TBS) (Figs. 1B–D).

We fixed and processed for electron microscopy only those slices demonstrating excellent physiology by the following criteria: (1) a gradually inclining I/O curve in response to incremental increases in stimulus intensity for both stimulating electrodes. (2) A stable baseline recording at both stimulating electrodes that was unchanged at the control site after induction of TBS-LTP. (3) TBS induced a significant increase in the slope of the field EPSP which was sustained for the duration of the experiment (Fig. 1).

## Fixation and Processing for ssTEM

Hippocampal slices with excellent physiology were fixed within a few seconds after the end of each experiment using a microwave enhanced procedure (Jensen and Harris, 1989), and processed for ssTEM (Harris et al., 2006). Briefly, the slices were fixed by immersion in mixed aldehydes (6% glutaraldehyde, 2% paraformaldehyde in 100 mM cacodylate buffer with 2 mM $CaCl_2$ and 4 mM $MgSO_4$) during 10 s of microwave irradiation to enhance diffusion of the fixative to the middle of the slice with a final temperature less than 35°C, and then were stored in the same fixative overnight at room temperature (Jensen and Harris, 1989). The slices were rinsed three times for 10 min each in 0.1M cacodylate buffer. Each slice was embedded in 7% agarose and manually trimmed under a dissecting microscope to the region of CA1 that contained both of the stimulating electrodes.

The fixed hippocampal slices were then vibra-sliced across their width at 70 μm thickness (Leica VT 1000S, Leica, Nussloch, Germany) and the vibra-slice was identified which showed a visible surface indentation of ~50 μm beneath the air surface that was caused by the stimulating electrode. This reference vibra-slice plus two located on either side were collected for each stimulating electrode (see black boxes in Fig. 1A). The 70-μm vibra-slices were immersed in 1% osmium and 1.5% potassium ferrocyanide in 100 mM cacodylate buffer for 10 min, rinsed five times in buffer, immersed in 1% osmium and microwaved (1 min ON-1 min OFF-1 min ON), cooled to 20°C, microwaved again (1 min ON-1 min OFF-1 min ON), and then rinsed five times for 2 min each in buffer and two times briefly in water. Slices were then transferred to graded ethanols (50, 70, 90, and 100%) containing 2% uranyl acetate and microwaved for 40 s for each transfer. Finally, slices were transferred through propylene oxide at room temperature and then embedded in LX112 and cured for 48 h at 60°C in an oven (Harris et al., 2006).

## Definition of "High Quality" Tissue Preservation

Test thin sections spanning the depth of the slice from air to net surface were evaluated from each experiment. Only those slices with a band of high quality tissue preservation spanning a depth of at least 100 μm were included in these analyses. High quality tissue preservation was defined by several criteria (See examples in Fig. 2): (1) the dendrites had well-defined microtubules that were relatively evenly spaced when viewed in crosssection. (2) Mitochondria were not swollen and cristae were discretely defined. (3) Most of the dendritic and axonal processes had clear cytoplasm and normal organelles indicating that few processes had been cut at the surface; compact black cytoplasm in shriveled processes or extremely swollen cytoplasm with distorted organelles were hallmarks of cut processes. (4) The postsynaptic densities had a compact thickness indicating the slice was not hypoxic at the time of fixation; excessively thick PSDs with "dangling" translucent lower edges were hallmarks of hypoxia in perfusion-fixed brain (Tao-Cheng et al., 2007). All of these criteria had to be met in both the control and TBS-LTP sides from the same slice. Of the 24 experiments that met the electrophysiology criteria established above, 16 were excluded because they did not meet these strict anatomical criteria.

## Three Dimensional Reconstructions and Measurements

Serial sections were cut from a small trapezoid positioned in regions located 150–200 μm lateral to each control or

TBS-LTP stimulating electrode (see black boxes in Fig. 1A) and 120–150 μm beneath the slices' air surface, and mounted on Pioloform-coated slot grids (Synaptek, Ted Pella). Sections were counterstained with saturated ethanolic uranyl acetate, followed by Reynolds lead citrate for 5 min each. Sections were imaged, blind as to condition, on a JEOL 1230 electron microscope with a Gatan digital camera at 5,000× magnification. Images from a series were given a five-letter code to mask the identity of experimental conditions in subsequent analyses.

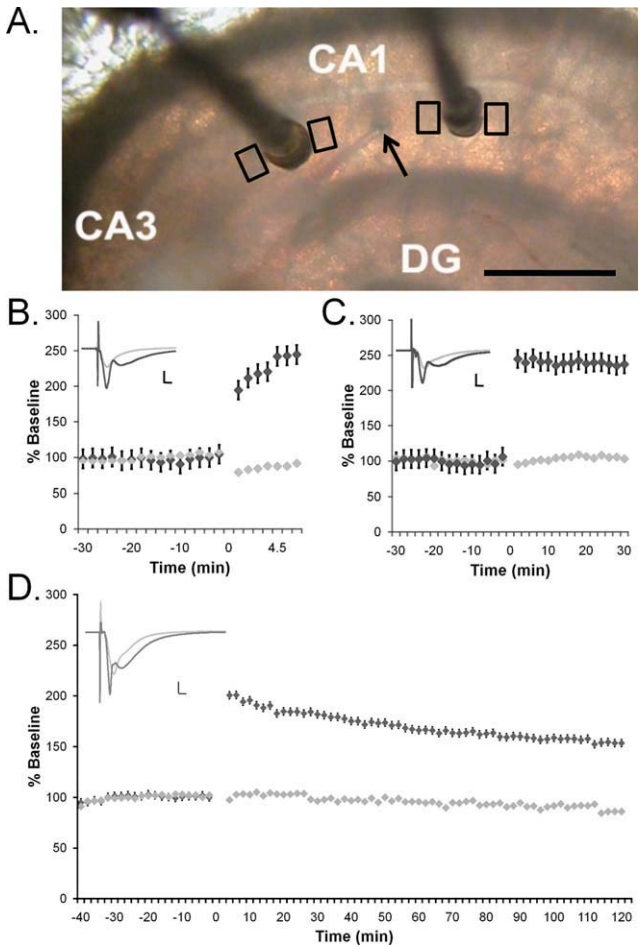


**FIGURE 1. Site-specific TBS-LTP in hippocampal slices from adult rats. (A) A single recording electrode (arrow) was positioned in the middle of *s. radiatum* midway between two stimulating electrodes (dark posts). Tissue for analyses was collected immediately adjacent to the stimulating electrodes (black boxes) after microwave-enhanced fixation. Scale bar = 500 μm. Theta burst stimulation (TBS) was delivered to one of the stimulating electrodes at time 0 to induce LTP (dark gray diamonds) while baseline stimulation was maintained at the other electrode (light gray diamonds). The responses were monitored for (B) 5 min ($n$ = 3 slices from three animals), (C) 30 min ($n$ = 3 slices from three animals), or (D) 2 h ($n$ = 2 slices from two animals) after the delivery of the first theta burst stimulation. Example waveforms for each time (insets) are an average of the pre-TBS and post-TBS responses at the control (light gray) and TBS-LTP (dark gray) sites. Scale bars = 5 mV/5 μs. [Color figure can be viewed in the online issue, which is available at wileyonlinelibrary.com.]**

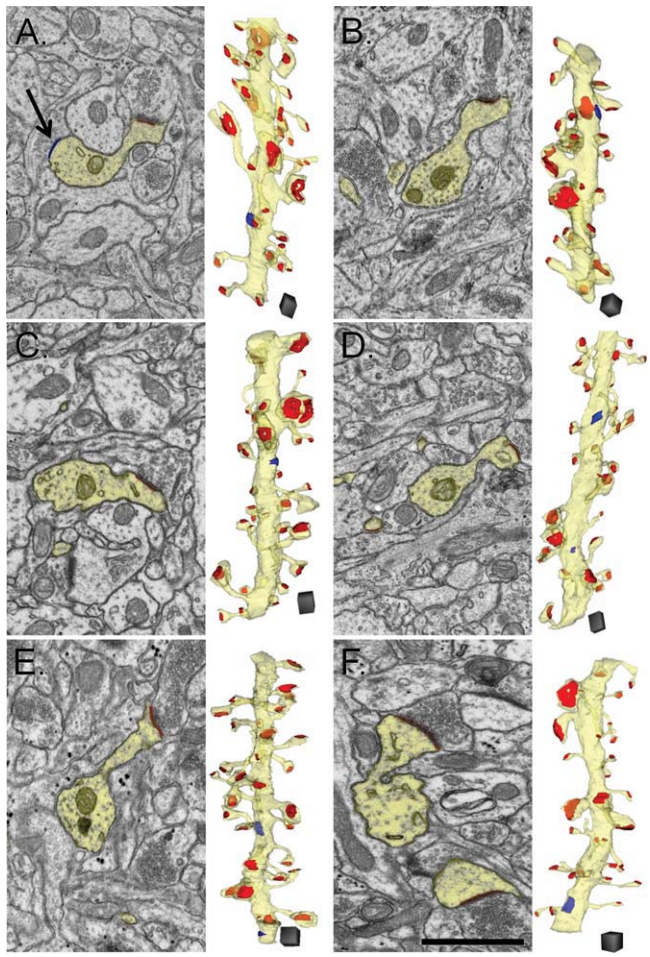


**FIGURE 2. Electron micrographs (EMs) of representative fields of neuropil illustrate high quality of tissue preservation from each time and condition. Sample dendrites and their spines were outlined and reconstructed in yellow. Asymmetric excitatory PSDs located on these dendrites were highlighted and reconstructed in red while symmetric shaft synapses were highlighted (arrow) and reconstructed in blue. Dendrites and surrounding neuropil in (A) a 5-min control, (B) a 5-min TBS-LTP series, (C) a 30-min control, (D) a 30-min TBS-LTP series, (E) a 2-h control, and (F) a 2-h TBS-LTP series. Scale bar = 1 μm. Scale cube = 0.5 μm on a side. [Color figure can be viewed in the online issue, which is available at wileyonlinelibrary.com.]**

The serial section images were aligned and dendrites were traced using the RECONSTRUCT™ software [available for free download at http://synapses.clm.utexas.edu (Fiala and Harris, 2001b; Fiala, 2005) Figs. 2 and 3]. Section dimensions were calibrated using a diffraction grating replica (Ernest Fullam, Latham, NY) imaged with each series and the cylindrical diameters method was used to compute section thickness by dividing the diameters of longitudinally sectioned mitochondria by the number of sections they spanned (Fiala and Harris, 2001a). The calculated section thicknesses ranged from 38 to 60 nm. Dendrite lengths were measured across serial sections using the z-trace tool in RECONSTRUCT™.

Synapse areas were measured taking into account the orientation in which they were sectioned. The area of a cross-sectioned synapse was calculated by measuring its length on each section and multiplying by section thickness and the number of sections it traversed. Enclosed areas of PSDs cut *en face* were measured on the section they appeared. Obliquely sectioned PSDs were treated as cross-sectioned if the presynaptic vesicles and pre- and postsynaptic membranes were clearly visible so that their size would not be over estimated by inadvertently including the depth of the PSD as surface area. Irregularly shaped synapses could span many serial sections and have cross-sectioned portions, *en face* portions, and portions that were cut obliquely; these were measured independently and then summed across the entire surface area of the PSD.

### Statistical Analyses

Statistical analyses were done in the STATICSTICA software package (StatSoft, Tulsa, OK). The variability between animals was addressed by first comparing TBS-LTP dendrites to their within slice controls and then combining the values for each condition (control or TBS-LTP) at each time and using either a two-way ANOVA or a nested hierarchical ANOVA with dendrite nested in condition and experiment to test whether TBS-LTP had a significant effect on dendrite, spine, or synaptic structural plasticity (see Supporting Information Table 1 for *n*'s in each condition). The number of dendrites and/or synapses analyzed is also indicated in each figure and figure legend. All data are expressed as mean ± S.E.M. or as described in specific figure legends.

## RESULTS

Site-specific LTP occurred only at the synapses stimulated by the electrode used to deliver TBS (see Methods above and Fig. 1), referred to as "TBS-LTP" in the text and figures. The large concentric bipolar stimulating electrodes were used to activate all of the axons in their immediate vicinity while providing input specificity when separated by more than 400 μm; we used 600–800-μm separation. Two hundred or more serial thin sections were cut in the middle of the optimal region described in the Methods above (see black boxes in Fig. 1A) and 120–150 μm beneath the slices' air surface. These sampling positions were chosen to maximize the number of axons that received TBS or control stimulation while minimizing the number of dendrites damaged or directly depolarized by the stimulating electrodes. Only slices demonstrating high-quality, input-specific LTP and outstanding tissue preservation were used for these studies (Fig. 2, see Methods for criteria).

### Sample Dendrites

Crosssectioned radial oblique dendritic segments that traversed at least 100 serial sections were selected for analysis based on the criteria of having a diameter ranging from 0.4 to 0.8 μm to assure that differences in dendrite caliber were not sufficient to impact spine density in control dendrites (Figs. 2 and 3, Supporting Information Fig. 1). All dendrites contained 7–22 crosssectioned microtubules and 1–4 mitochondria along the length of the reconstructed segments. No spines contained mitochondria or microtubules.

Spine densities at all time points and experimental conditions were within the range of those measured along oblique CA1 dendrites in adult, perfusion-fixed hippocampus (average = 3.49 ± 0.31 spines/μm and range = 2.55–5.25 spines/μm). At 5 min, the 20 dendrites from 7 ssTEM series measured 0.56 ± 0.004 μm in diameter, 9.67 ± 0.36 μm in length and had 583 excitatory synapses and 40 inhibitory synapses. At 30 min, the 25 dendritic segments from 6 ssTEM series measured 0.59 ± 0.004 μm in diameter and 7.89 ± 0.25 μm in length and had 672 excitatory synapses and 31 inhibitory synapses. At 2 h, the 18 dendrites from 4 ssTEM series measured 0.55 ± 0.004 μm in diameter and 9.42 ± 0.76 μm in length and had 636 excitatory synapses and 25 inhibitory synapses. Thus, the sampled dendritic segments and synapses were of comparable dimensions and quantity and there was no significant correlation between dendrite diameters or lengths with any of the measured parameters of spine density, PSD area, or polyribosome frequency reported below.

### Rapid Synaptogenesis Following Induction of TBS-LTP

First we tested whether synaptogenesis occurred along mature CA1 dendrites after induction of TBS-LTP. Synaptogenesis is characterized by the emergence of "transitional structures" which have been found to become spines or to be eliminated in both immature and mature hippocampus (Fiala et al., 1998; Engert and Bonhoeffer, 1999; Maletic-Savatic et al., 1999). Transitional structures include asymmetrical shaft synapses on spiny dendritic segments, stubby spines, nonsynaptic filopodia originating from dendritic shafts or from the heads of dendritic spines (Richards et al., 2005) and multisynaptic spines (Figs. 4A–Dii). Transitional structures occurred with a frequency of 0–0.92 per micron length of dendrite and constituted 8% of all the synapses. Because of the low frequency of transitional structures, data were plotted as the change in density between TBS-LTP and control at each time point to illustrate the direction and magnitude of the change (Fig. 4E). Specifically, more asymmetric shaft synapses and stubby spines appeared transiently at 5 min, and nonsynaptic filopodia were increased at 30 min (Fig. 4E). There was no significant change in multisynaptic spine frequencies (Fig. 4E). All transitional structures were equal to control levels by 2 h after induction of TBS-LTP (Fig. 4E). These findings suggest that synaptogenesis occurred early after TBS-LTP but was balanced by elimination or conversion of transitional structures into more typically mature spines by 2 h as discussed below.

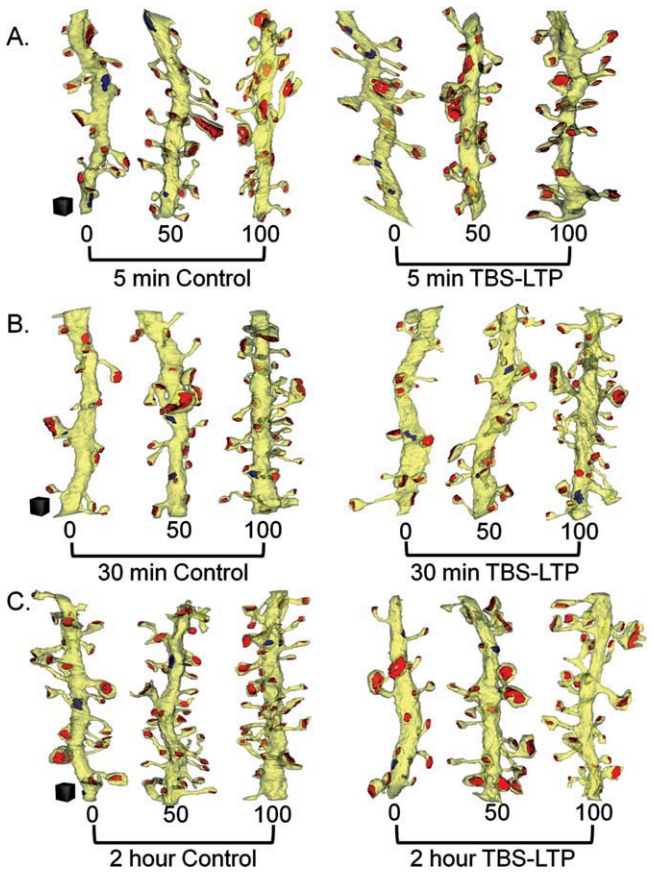


## Changes in Typical Dendritic Spine Density Following Induction of TBS-LTP

When reconstructed in 3D, most "typical" spines in mature hippocampus can be described as thin (Fig. 5A, Supporting Information Figs. 2A–D), mushroom (Fig. 5B, Supporting Information Figs. 2E–H), or branched, where different branches could be thin or mushroom shaped and always synapsed with different axons (Fig. 5C, Supporting Information Figs. 2I–L). The distribution of spine density for each dendrite varied across time and condition (Figs. 3 and 5D).

Smaller spines are thought to be more labile under a variety of developmental and experimental conditions (Bourne and Harris, 2007). We tested this hypothesis for TBS-LTP on mature CA1 dendrites by comparing the spine head diameters to determine whether changes in density were specific to spines of particular sizes. Spine head diameters were measured at the widest part parallel to the PSD (Figs. 5Ai,Bi). Spines were grouped as "small thin spines" with head diameters less than

**FIGURE 3. Example reconstructed dendritic segments from each condition, ranked according to spine density and displayed at comparable percentile ranks of 0, 50 and 100 from the Control or TBS-LTP sites at (A) 5 min, (B) 30 min, or (C) 2 h after induction of TBS-LTP. All of the excitatory (red) and inhibitory (blue) synapses were reconstructed on each dendritic segment. Scale cubes equal 0.5 µm on a side and were matched for all conditions and times. [Color figure can be viewed in the online issue, which is available at wileyonlinelibrary.com.]**

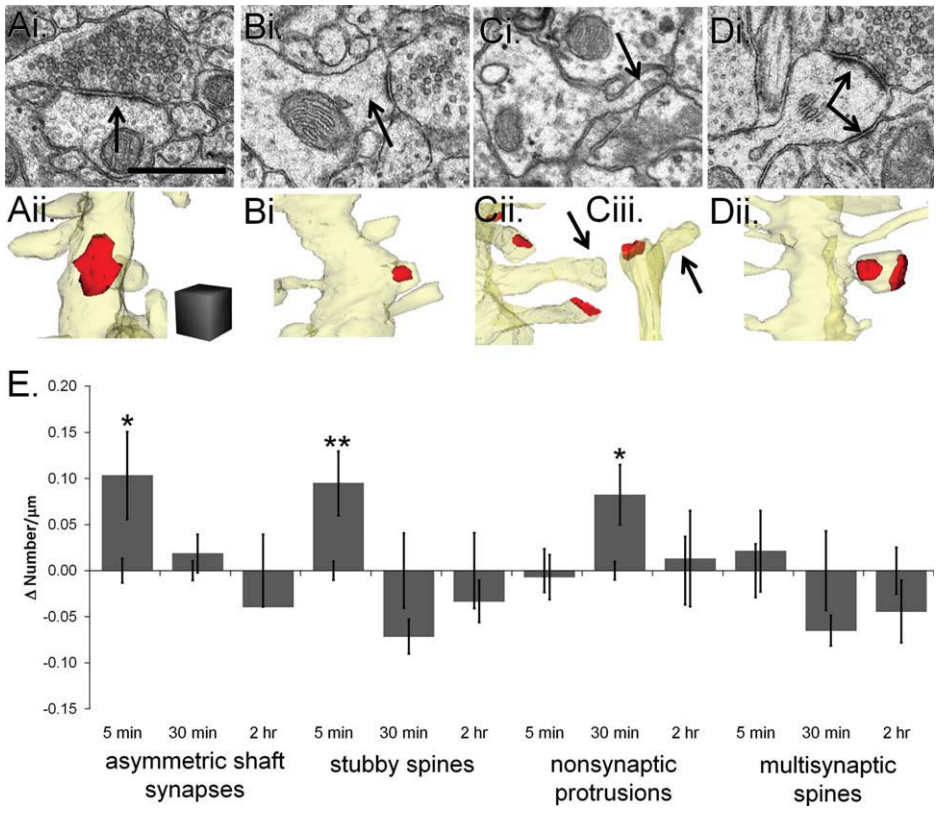


**FIGURE 4.**

0.45 μm, "medium thin spines" with head diameter greater than 0.45 μm but less than 0.6 μm, and "mushroom spines" with head diameters greater than 0.6 μm (Harris et al., 1992; Yankova et al., 2001). Curiously, the density of the smallest thin spines with head diameters <0.45 μm was greatest along the control dendrites at 2 h (Fig. 5E; Supporting Information Fig. 5A), suggesting an ongoing spine recovery in the slices. Nevertheless, these small thin spines were selectively lowered at 2 h after the induction of TBS-LTP (Fig. 5E, $P < 0.05$), supporting the hypothesis that they were the most labile.

## Enlargement of Average PSD Area by 2 h After Induction of TBS-LTP

One explanation for the reduction in small spines by 2 h after induction of TBS-LTP is that an alteration in spine turnover occurred through the stabilization and enlargement of a subset of spines at the expense of ongoing spine formation. To test this hypothesis, we compared spine head diameter and PSD areas at all time points (Fig. 6A, black line, 6B). The surface areas of the postsynaptic densities (PSD) were measured across serial sections and PSDs were categorized as macular or perforated depending on whether an electron lucent region separated the PSD into one or more parts, or created a hole in the center of the PSD (Supporting Information Figs. 2A–H).

We reconstructed the surface area of each PSD on every spine for a total of 1,891 synapses. Although there was a wide range in spine head diameters at each time point, there was no significant change in average spine head size with TBS-LTP (Fig. 6C). The PSDs ranged in size from 0.01 to 0.86 $\mu m^2$ (Fig. 6D). There was no significant difference in the relative frequencies of macular or perforated PSDs at any time point. We found that the average PSD area was enlarged on spines of all sizes at 2 h after the induction of TBS-LTP (Fig. 6E, $P < 0.01$, $P < 0.01$, $P < 0.05$, respectively), but not on spines at 5 or 30 min. The PSD area on transitional spines did not differ significantly at any time or condition (Supporting Information Fig. 3). These data support the hypothesis that the initial increases in synaptic strength are due to unsilencing of synapses (Kerchner and Nicoll, 2008), trafficking of AMPA receptors into preexisting "slots" in the PSD (Lisman and Raghavachari, 2006), or alterations in presynaptic release probability (Zakharenko et al., 2001; Enoki et al., 2009). Later, by 2 h after the induction of TBS-LTP, a fraction of all the synapses on typical spines of all sizes underwent enlargement.

**FIGURE 4. Transitional structures emerged soon after the induction of TBS-LTP. (Ai) EM (arrow) and (Aii) 3D reconstruction of an asymmetric excitatory shaft synapse, which was unambiguously identified by comparing the typical PSD thickness with neighboring spine PSDs and confirming the identity by following the axon until it synapsed on a dendritic spine. Scale bar and cube = 0.5 μm on a side for A–D. (Bi) EM (arrow) and (Bii) reconstruction of a stubby spine. Reconstruction of a nonsynaptic filopodia emerging from (Ci, Cii) a dendritic shaft (arrow), or (Ciii) a dendritic spine (arrow). (D) EM of a spine with two synapses (arrows) formed by different presynaptic axons. (Di) Reconstruction of the same multisynaptic spine. (E) To visualize changes in transitional structures, we subtracted the mean control value from the mean TBS-LTP-value for each time (Δ Number/μm) and plotted here the differences relative to the control values which were normalized to zero while maintaining the error bars from statistical analyses of the absolute mean values for both control and TBS-LTP. Asymmetric shaft and stubby spine synapses were increased at 5 min and more nonsynaptic filopodia were present at 30 min (*$P < 0.05$, **$P < 0.01$). There was no significant change in multisynaptic spines at any time following TBS-LTP induction. [Color figure can be viewed in the online issue, which is available at wileyonlinelibrary.com.]**

## Association of Polyribosomes With Sustained Excitatory Synapse Enlargement

Local protein synthesis is required for maintenance of LTP (Frey and Morris, 1997; Aakalu et al., 2001; Steward and Schuman, 2001; Sutton and Schuman, 2005) and is evidenced ultrastructurally by polyribosomes (Figs. 7A–C, Supporting Information Fig. 4). Previous work demonstrated a redistribution of polyribosomes from dendritic shafts into spines with larger PSDs at 2 h after induction of LTP by tetanic stimulation (tetanic-LTP) in hippocampal slices from young (Ostroff et al., 2002) and mature (Bourne et al., 2007b) rats. We wanted to learn when and where polyribosomes were upregulated following induction of TBS-LTP. Polyribosomes were identified by the presence of three or more dark round ribosomes, each ~18–25 nm in diameter with a gray fuzz connecting them (Ostroff et al., 2002; Bourne et al., 2007b). An individual proteasome measures about 20 by 45 nm (Medalia et al., 2002; Robinson et al., 2007) and a single ribosome might be confused with it or other similarly sized macromolecular complexes; hence only clusters containing three or more ribosomes were included in these analyses. Polyribosomes assumed a variety of shapes including spirals, linear strings, or spherical or irregularly shaped clusters. Polyribosomes usually occupied just one section, although those having more than 10 ribosomes sometimes spanned two or three sections; all polyribosomes were followed across serial thin sections to distinguish them from other dark staining structures, such as membranes (Supporting Information Fig. 4).

The frequency of polyribosomes ranged from 0 to 2.2 per micron length of dendrite (Fig. 7D). Overall, 4–10% of all spines contained polyribosomes. Under control conditions, there was a constitutive elevation in polyribosomes in the dendritic shaft and at the base of and in the heads and necks of dendritic spines across time in vitro (Fig. 7E; Supporting Information Fig. 5B), suggesting that baseline stimulation may recruit local protein synthesis to promote the ongoing recovery of synapses in hippocampal slices (as discussed above and shown in Supporting Information Fig. 5A). TBS-LTP interacted with the formation of polyribosomes in the dendritic shaft and in spine heads and necks in several interesting ways. First, by 5 min after TBS there was a marked elevation in the frequency of polyribosomes in spine heads and necks, relative to the controls at that time point (Fig. 7E, $P < 0.01$). At 30 min the control elevation in polyribosomes was unaffected by

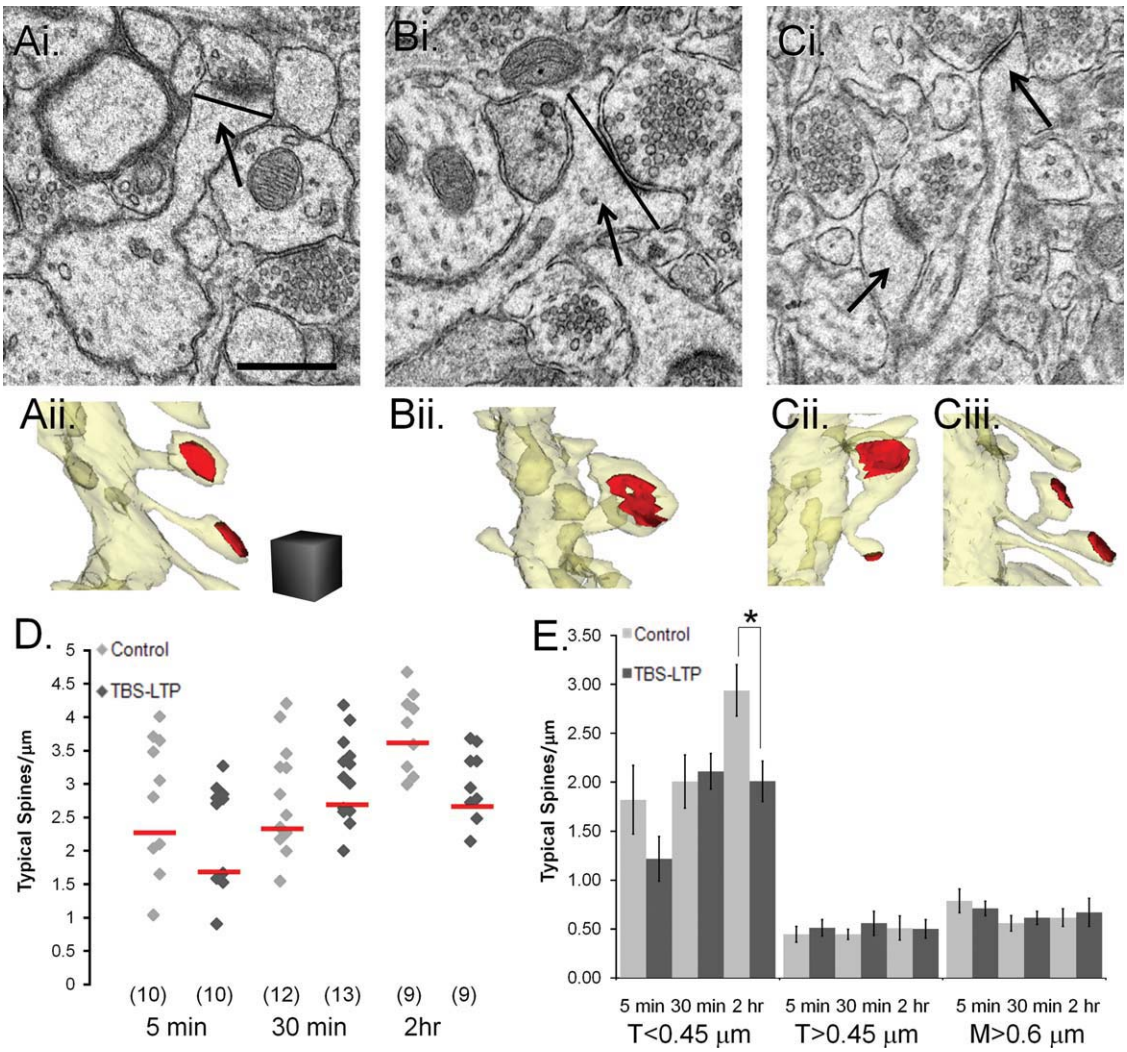


**FIGURE 5. A decrease in the smallest thin spines accounted for a TBS-LTP specific reduction in dendritic spine density at 2 h. (Ai) EM of a thin spine (arrow). Scale bar = 0.5 µm for all EMs. (Aii) Reconstruction of a dendritic segment where two thin spines were illustrated with each of their PSDs reconstructed in red. Scale cube = 0.5 µm on a side for all reconstructions. (Bi) EM (arrow) and (Bii) reconstruction of a mushroom spine. Black lines in (Ai) and (Bi) indicate where the measurements of spine heads were obtained at their greatest width parallel to the PSD. (Ci) EM of both heads of a branched spine, where the branch point was visualized on adjacent serial sections (see Supporting Information Figs. 2I–L). (Cii) Reconstructed branched spines with one mushroom head and one thin head and (Ciii) with two thin heads. (D) The distribution in spine density of control dendrites (light gray diamonds) and TBS-LTP dendrites (dark gray diamonds) is plotted for each time. The red horizontal lines represent the means ($n$ = number of dendrites). (E) Comparison of typical spine frequency based on head diameters where there was a significant decrease in thin <0.45 µm spines at the 2-h time point (*$P < 0.05$) but no change in larger spines or at other time points. [Color figure can be viewed in the online issue, which is available at wileyonlinelibrary.com.]**

TBS-LTP. However, by 2 h, TBS-LTP resulted in a marked reduction in the polyribosomes in the heads and necks of dendritic spines, back to the control levels measured at 5 min (Fig. 7E, $P < 0.01$). There were also fewer polyribosomes in dendritic shafts by 2 h (Fig. 7E, $P < 0.05$).

Next we tested whether there was a preferential distribution of polyribosomes to enlarged spines during TBS-LTP (Fig. 7F). Under the control conditions spine size did not differ significantly whether or not they contained a polyribosome, suggesting that these polyribosomes were not synthesizing proteins specifically involved in spine enlargement. In contrast, at all times after induction of TBS-LTP, spines that contained polyribosomes had significantly larger heads (Fig. 7F, $P < 0.05$). These results suggest that a different set of proteins relative to controls were being synthesized to support spine enlargement following TBS-LTP.

In addition, we tested whether the average PSD area was larger on spines with polyribosomes. Again, under the control conditions PSD size did not differ whether or not the spine contained a polyribosome, suggesting that these polyribosomes were not synthesizing proteins specifically involved in synapse enlargement. In contrast, at 5 min and 2 h after induction of

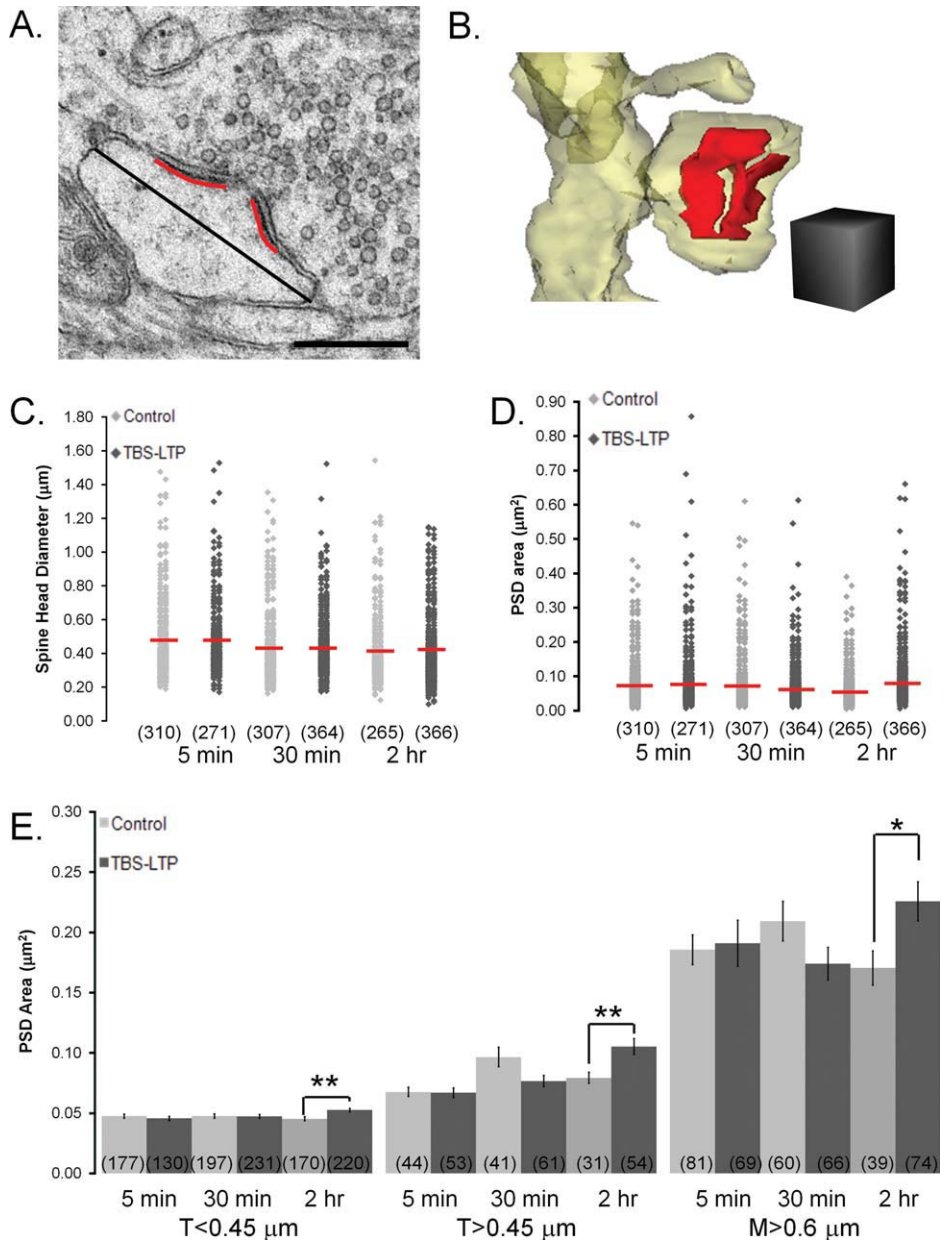


**FIGURE 6. PSD enlargement by 2 h after induction of TBS-LTP without significant change in spine head diameter. (A) EM of a dendritic spine head from the 2 h TBS-LTP condition, with a red line along a cross-sectioned PSD length showing a gap where it is perforated by an electron lucent region. The black line indicates spine head diameter measurements taken at the widest part of the dendritic spine parallel to the PSD. Scale bar = 0.5 μm. (B) Reconstruction of the perforated PSD (red) on the mushroom spine depicted in (A). Scale cube = 0.5 μm on a side. (C) Distribution of all spine head diameters with red horizontal lines indicating means for each time point for control (light gray diamonds) and TBS-LTP (dark gray diamonds) conditions (*n* = number of spines). Average spine head diameter was not significantly changed after the induction of TBS-LTP. (D) The PSD area of every excitatory synapse was plotted at 5 min, 30 min, and 2 h to visualize the range in size across control (light gray diamonds) and TBS-LTP (dark gray diamonds) dendrites. Red horizontal lines indicate the mean for each time and condition (*n* = number of synapses). (E) At 2 h average PSD area was increased for spines of all sizes (*n* = number of synapses) (**P* < 0.05, ***P* < 0.01). [Color figure can be viewed in the online issue, which is available at wileyonlinelibrary.com.]**

TBS-LTP, PSDs were larger on spines that contained polyribosomes (Fig. 7G, $P < 0.01$).

These findings suggest that by 5 min after the induction of TBS-LTP, mRNAs were immediately "unmasked" in large spines that already had large PSDs. The findings further suggest that by 30 min, newly unmasked mRNAs also appeared in larger spines that did not yet have larger PSDs. By 2 h after induction, further enlargement of all PSDs resulted in the preferential location of polyribosomes in enlarged spines with enlarged PSDs. Since overall, the density of polyribosomes was

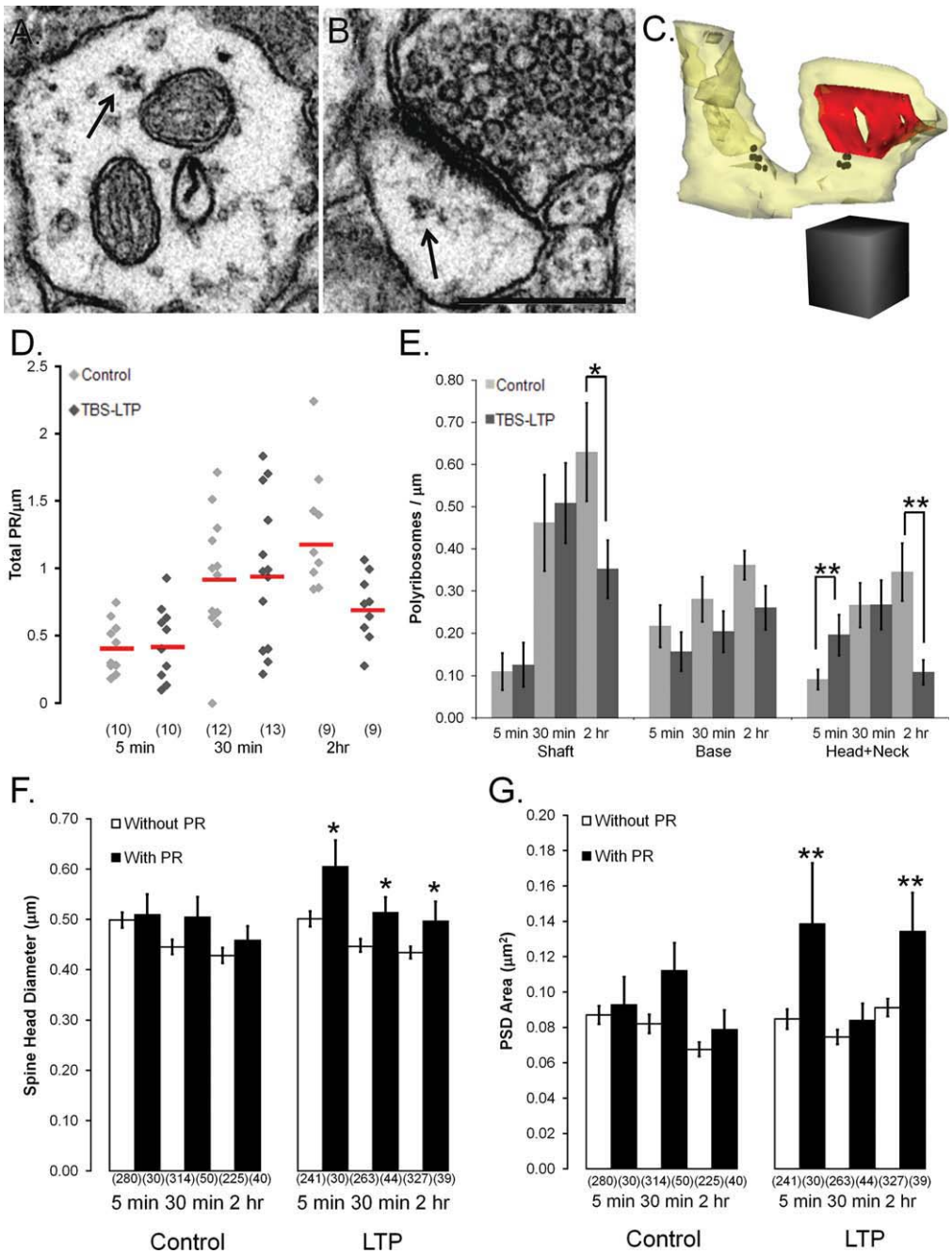


**FIGURE 7.** **Timing of changes in the density and location of polyribosomes after induction of TBS-LTP. Polyribosomes had three or more individual ribosomes with opaque centers (~15–25 nm) surrounded by lighter irregular edges as illustrated (A) in a dendritic shaft (arrow) and (B) in a spine head (arrow). (See also Supporting Information Fig. 4). Scale bar = 0.5 µm. (C) Reconstruction of a mushroom spine with a large perforated PSD (red) and containing a polyribosome (black spheres) at the base of the spine and a polyribosome in its head. Scale cube = 0.5 µm on a side. (D) The distribution of total polyribosome density for control (light gray diamonds) and TBS-LTP (dark gray diamonds) dendrites was plotted for each time and condition. Red horizontal lines indicate means for each population of dendrites ($n$ = number of dendrites). (E) Relative to controls, polyribosomes were elevated in spine heads and necks at 5 min after induction of LTP but were reduced in the dendritic shaft and in spine heads and necks by 2 h (*$P < 0.05$; **$P < 0.01$). (F) Spines with polyribosomes had significantly larger heads at all times after induction of TBS-LTP ($P < 0.05$) ($n$ = number of spines). (G) At 5 min and 2 h after the induction of LTP, spines with polyribosomes had significantly larger PSDs (**$P < 0.01$) whether the polyribosomes were in the head, neck or base of the spine ($n$ = PSDs on the same spines as in F). [Color figure can be viewed in the online issue, which is available at wileyonlinelibrary.com.]**

decreased at 2 h relative to earlier time points, the data suggest that polyribosomes and their associated mRNAs were "used up" by 30 min in the heads of potentiated spines undergoing synapses enlargement and replenished from the dendritic shafts into spines with further enlarged PSDs by 2 h. Further work is needed to determine whether replenishment from the soma is required to sustain local translation at later times after the induction of TBS-LTP.

### Balancing "Inhibitory" Symmetric Synapse Size and Number

GABAergic synapses have been found to increase in the mature barrel cortex of mice following prolonged whisker stimulation (Knott et al., 2002). It is not known, however, whether synaptic structure of inhibitory synapses changes when LTP is produced at excitatory synapses. We identified presumptive inhibitory synapses by their symmetric pre- and postsynaptic densities and pleiomorphic vesicles in the presynaptic axonal bouton [Fig. 8A, Supporting Information Figs. 2A–D (Harris et al., 1985; Peters et al., 1991)]. Symmetric synapses displayed some variability in their opacity (Colonnier, 1968), hence as an additional measure we looked for the consistent appearance of symmetric synapses at other boutons along the same axon. Symmetric synapse surface areas were measured where the slightly widened, uniform cleft was obvious across serial sections (Fig. 8B).

We quantified the relative frequencies of symmetric synapses along each of the reconstructed dendrites (Figs. 3 and 8C), and found that there was a significant drop in the number of symmetric synapses per unit length of dendrite at 2 h after the induction of TBS-LTP (Fig. 8D, $P < 0.01$). Like the asymmetric synapses discussed above, there was also a marked increase in the average surface area of these symmetric synapses at 2 h after the induction of TBS-LTP (Fig. 8F, $P < 0.001$). This decrease in the frequency of symmetric synapses coupled with enlargement of their size could serve to maintain a balance in the inhibitory input on a dendritic segment.

### Absence of Polyribosomes Near Shaft Synapses

We wanted to determine if the increase in the surface area of symmetric synapses at 2 h after induction of TBS-LTP was linked to nearby protein synthesis in the dendritic shafts. Figure 9C illustrates how we performed this analysis. All 63 dendrites were examined for the locations of symmetric synapses with respect to the shaft polyribosomes. Most of the polyribosomes in the dendritic shaft were located more than 2 μm away from the synapse, a distance comparable to spine length (Fig. 9A) and only one example was found where a polyribosome was within 0.1 μm of a symmetric synapse (Fig. 9B). To determine whether the absence of polyribosomes was specific to symmetric synapses or a feature of all shaft synapses, we performed an identical analysis on asymmetric shaft synapses. Again, all 63 dendrites were examined for the location of asymmetric synapses with respect to the shaft polyribosomes. There were no examples of a polyribosome within 0.1 μm of an asymmetric shaft synapse (Fig. 9D). These findings suggest that local protein synthesis in the immediate vicinity of symmetric or asymmetric shaft synapses may not be as important as for spine synapses. The compartmentalization of synapses located on dendritic spines may necessitate their capture or recruitment of mRNAs and polyribosomes.

### Balancing Synapse Size and Number

The decrease in small spines and enlargement of PSDs by 2 h after the induction of TBS-LTP suggests that dendrites may have a set amount of synaptic resources that are distributed to spines based on the level of synaptic strength. Synaptic components can be exchanged between spines along a dendrite, and larger synapses tend to capture more molecules than smaller synapses (Gray et al., 2006; Park et al., 2006; Tsuriel et al., 2006; Harvey et al., 2008; Rose et al., 2009; Zhong et al., 2009). If the amount of synaptic components available within a dendrite remains stable, then the total amount of synapse area should be constant per length of dendrite.

To test this hypothesis, we summed synaptic areas for all asymmetric or symmetric synapses along each dendritic segment and divided by segment length (Fig. 10A). The summed PSD area for asymmetric synapses positively correlated with total dendritic length for all dendrites across conditions and time points (Fig. 10B, $P < 0.001$). Furthermore, the correlation between summed asymmetric PSD area and dendrite length was sustained despite a marked increase in average PSD size and lower spine number at 2 h after the induction of TBS-LTP (Fig. 10C, $r = 0.8$ control, $P < 0.05$; and $r = 0.8$ TBS-LTP, $P < 0.01$). In contrast, there was no significant correlation between summed surface area of symmetric synapses and the length of the analyzed dendritic segments (Fig. 10 B). Since symmetric synapses are relatively sparse in *s. radiatum*, reconstruction of longer segments or more proximal dendrites where symmetric synapses dominate might be needed to detect such correlation.

The average summed synaptic surface area per micron length of dendrite remained stable across conditions and time for both asymmetric and symmetric synapses, indicating a coordinated response after the induction of TBS-LTP (Fig. 10D). These findings suggest that the overall amount of excitatory and inhibitory input onto a mature dendritic segment is preserved following induction of TBS-LTP even when the size of individual synapses is shifted as some synapses are enlarged while others shrink or are lost.

## DISCUSSION

Three-dimensional reconstructions of mature CA1 dendrites revealed a remarkable balancing between synapse size and number for both excitatory and inhibitory synapses following induction of LTP. Figure 11 illustrates the sequence of structural events. Over all conditions, the absolute spine and synapse

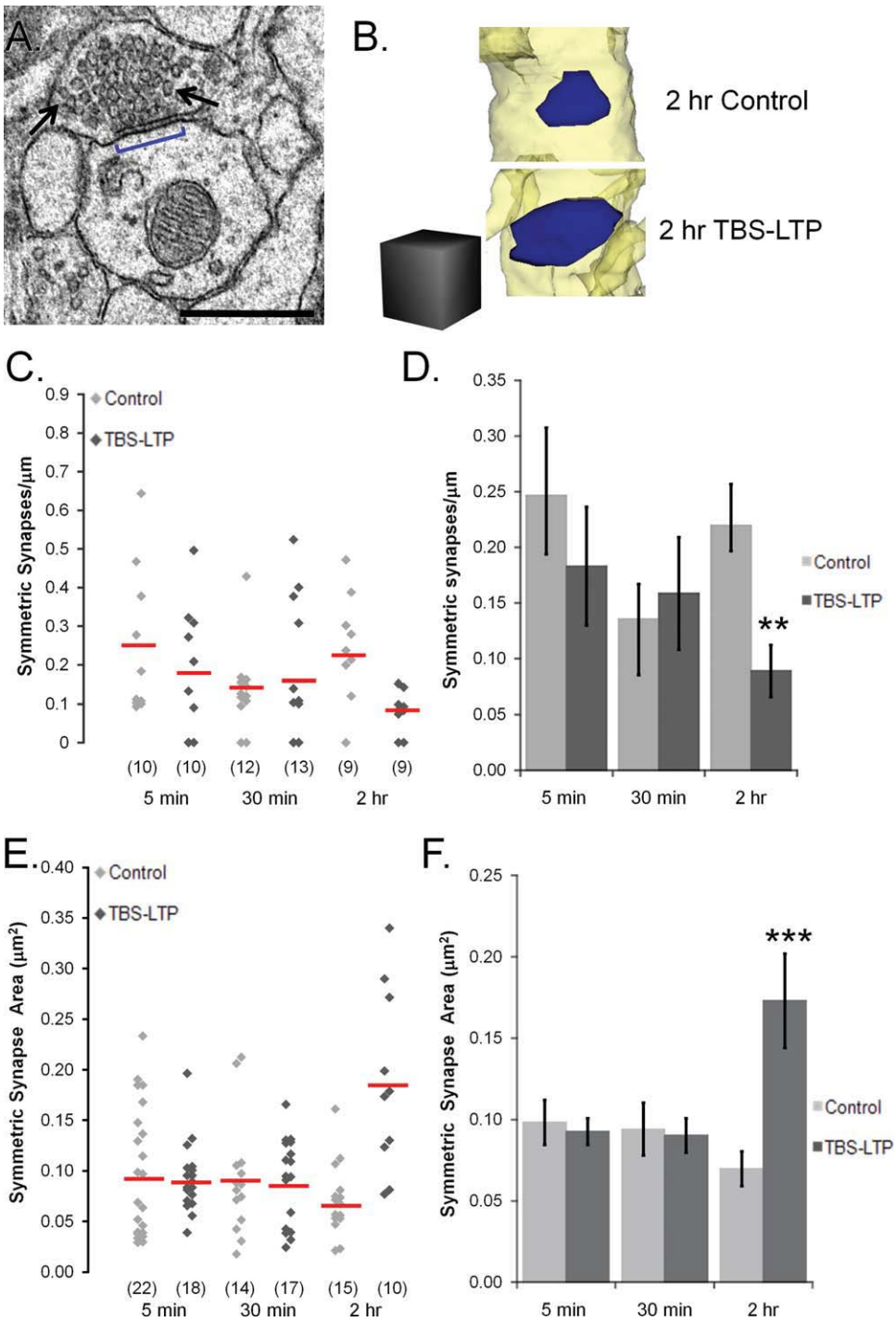


**FIGURE 8. Reduced frequency and enlargement of symmetric synapses at 2 h after TBS-LTP was produced at excitatory synapses in *s. radiatum*. (A) EM of a symmetric synapse (blue bracket) with small pleiomorphic presynaptic vesicles (arrows). Scale bar = 0.5 µm. (B) Reconstructions of symmetric synaptic surface areas (blue) from 2 h control and TBS-LTP dendrites. Scale cube = 0.5 µm on a side. (C) The distribution of symmetric synapse density was plotted for every control (light gray diamonds) and TBS-LTP (dark gray diamonds) and red horizontal lines indicate means for each time point and condition ($n$ = number of dendrites). (D) Relative to controls, fewer symmetric synapses occurred at 2 h (**$P < 0.01$) with no significant change at 5 or 30 min after TBS. (E) The surface area of each symmetric synapse on control (light gray diamonds) and TBS-LTP (dark gray diamonds) dendrites was plotted with red lines indicating means for each time point and condition ($n$ = number of synapses). (F) There was an increase in the surface area of symmetric synapses (***$P < 0.001$) at 2 h after the induction of TBS-LTP. [Color figure can be viewed in the online issue, which is available at wileyonlinelibrary.com.]**

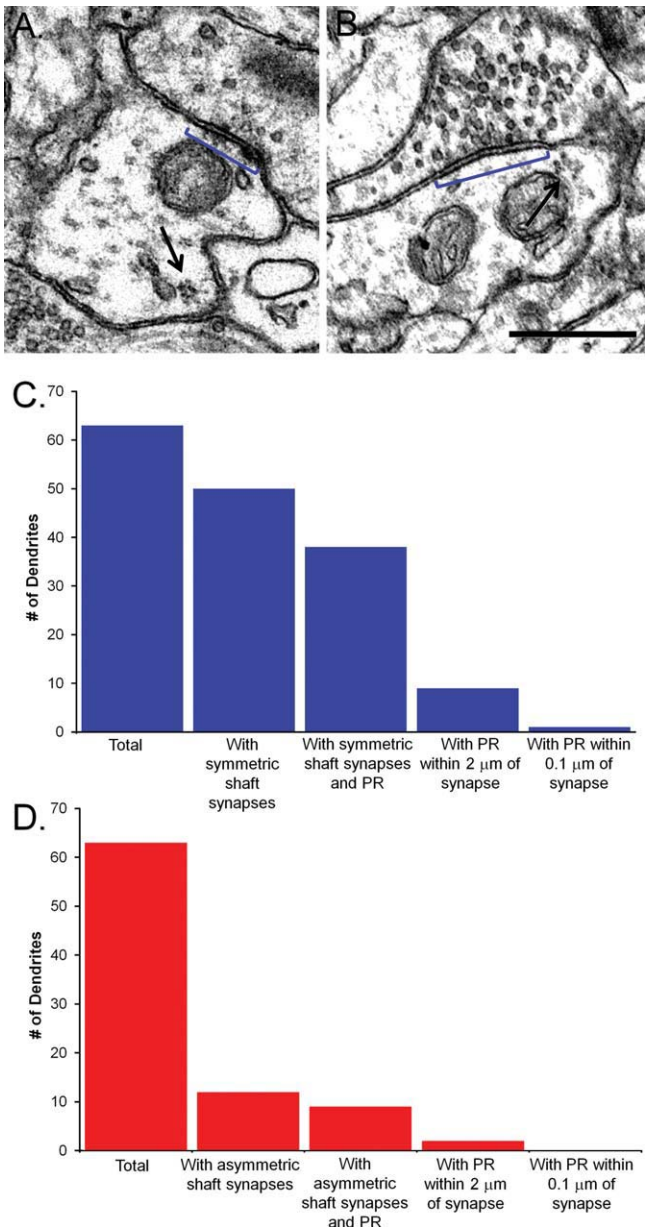


**FIGURE 9. Polyribosomes were not associated with symmetric or asymmetric shaft synapses in the middle of *s. radiatum*. (A) An EM of a symmetric synapse (blue bracket) with a polyribosome (arrow) located in the dendritic shaft >0.1 μm away. (B) An EM of the one symmetric synapse (blue bracket) with a polyribosome (arrow) located <0.1 μm away. Scale bar = 0.5 μm. (C) All dendrites ($n$ = 63) were divided into those with symmetric synapses ($n$ = 50) and then further separated into those with symmetric synapses and shaft polyribosomes ($n$ = 38). Dendrites that had polyribosomes within 2 μm of a symmetric synapse ($n$ = 9) were finally parsed down to one dendrite that had a polyribosome within 0.1 μm of a symmetric synapse, the cutoff distance that was used to assign a polyribosome to a dendritic spine. (D) All dendrites ($n$ = 63) were divided into those with asymmetric shaft synapses ($n$ = 12) and then further separated into those with asymmetric shaft synapses and shaft polyribosomes ($n$ = 9). There were two dendrites that had polyribosomes within 2 μm of an asymmetric shaft synapse but there were not any asymmetric shaft synapses that had a polyribosome within 0.1 μm. [Color figure can be viewed in the online issue, which is available at wileyonlinelibrary.com.]**

numbers were within the range found along mature dendrites from perfusion-fixed hippocampus (Kirov et al., 1999, 2004b; Bourne et al., 2007a). Synaptogenesis marked by the formation of additional asymmetric shaft synapses, stubby spines, and nonsynaptic filopodia was initiated specifically within 30 min after the induction of TBS-LTP (Figs. 11A–B′). By 2 h, the smallest, presumably most labile synapses were markedly reduced relative to dendrites receiving control stimulation (Figs. 11C,C′). Whether this form of plasticity resulted from elimination of small spines or prevention of their constitutive formation during 2 h of control stimulation remains to be determined.

Polyribosomes were elevated immediately in spines with large heads and PSDs (Fig. 11A′). Control stimulation resulted in a constitutive increase in polyribosomes by 2 h, perhaps in support of the ongoing formation of small spines. In contrast, TBS-LTP resulted in a substantial loss of polyribosomes overall, but a significant targeting of those that remained to large spines with enlarged PSDs (Figs. 11C,C′). This finding suggests that TBS-LTP uses newly synthesized proteins to build larger PSDs and subsequently replenishes or redirects mRNAs and polyribosomes to those spines with enlarged heads and PSDs. Excitatory and inhibitory synapses were sufficiently enlarged by 2 h after induction of TBS-LTP to counterbalance the lower densities of small spines and inhibitory synapses (Figs. 11C,C′). These results support a model of clustered synaptic plasticity that involves coordinated structural plasticity along mature CA1 dendrites which may be mediated by a redistribution or sharing of resources among neighboring synapses (Govindarajan et al., 2006; Harvey and Svoboda, 2007; Harvey et al., 2008; Losonczy et al., 2008; Makara et al., 2009).

Filopodia and other transitional structures such as stubby spines and excitatory asymmetric shaft synapses are prevalent during synaptogenesis along developing dendrites (Dailey and Smith, 1996; Fiala et al., 1998; Harris, 1999; Yuste and Bonhoeffer, 2004; Richards et al., 2005), but have been observed in the mature hippocampus only under conditions of homeostatic plasticity induced by synaptic inactivation (Petrak et al., 2005) or preparation of hippocampal slices (Kirov et al., 1999, 2004b). Potentiation of a single synapse on a cultured neuronal dendrite lowers the threshold for LTP induction at neighboring synapses (Harvey and Svoboda, 2007) and encourages local emergence of new spines (Engert and Bonhoeffer, 1999; Maletic-Savatic et al., 1999; Ostroff et al., 2002; Nagerl et al., 2004, 2007; De Roo et al., 2008) and loss of more distal or nonactivated spines (Engert and Bonhoeffer, 1999; Nagerl et al., 2004, 2007; De Roo et al., 2008). The immediate increase in transitional synaptogenic structures after induction of TBS-LTP suggests that spine turnover initially favors spinogenesis along mature CA1 dendrites. Since overall spine density did not increase, synapse elimination must have also occurred as LTP was established.

Slicing-induced spinogenesis was less robust in the hippocampal slices prepared at room temperature in the current study compared to previous slices prepared with ice-cold ACSF (Kirov et al., 1999, 2004b). Nevertheless, the small, apparently

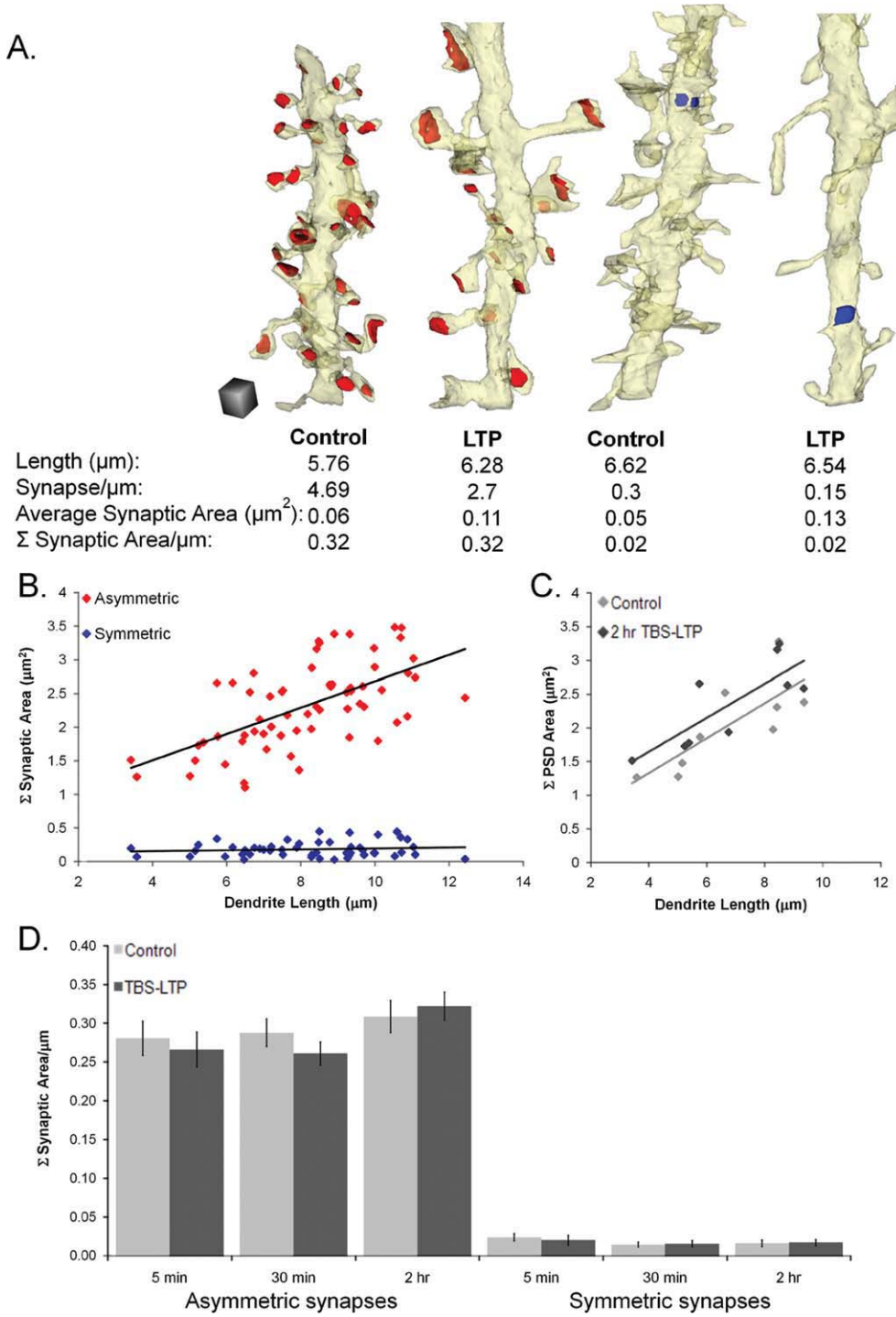


**FIGURE 10.** Balancing total PSD area along reconstructed dendrites. (A) Reconstructions of control and TBS-LTP dendrites cropped to approximately equal lengths demonstrate equal summed asymmetric or symmetric synaptic areas per micron despite large differences in average synapse size and density. Scale cube = 0.5 µm on each side. (B) Summed asymmetric PSD area was well correlated with dendritic length across all dendrites (red diamonds, $n = 63$ dendrites; $r = 0.6$, $P < 0.001$) but summed surface area of symmetric synapses was not (blue diamonds; $r = 0.12$, n.s.). (C) This correlation applied also to control (light gray diamonds; $r = 0.8$, $P < 0.05$) and LTP (dark gray diamonds; $r = 0.8$, $P < 0.01$) dendrites at 2 h after the induction of TBS-LTP. (D) Average summed asymmetric or symmetric surface area per micron length of dendrite was the same for dendrites across all time points in the control and TBS-LTP conditions ($P > 0.8$). [Color figure can be viewed in the online issue, which is available at wileyonlinelibrary.com.]

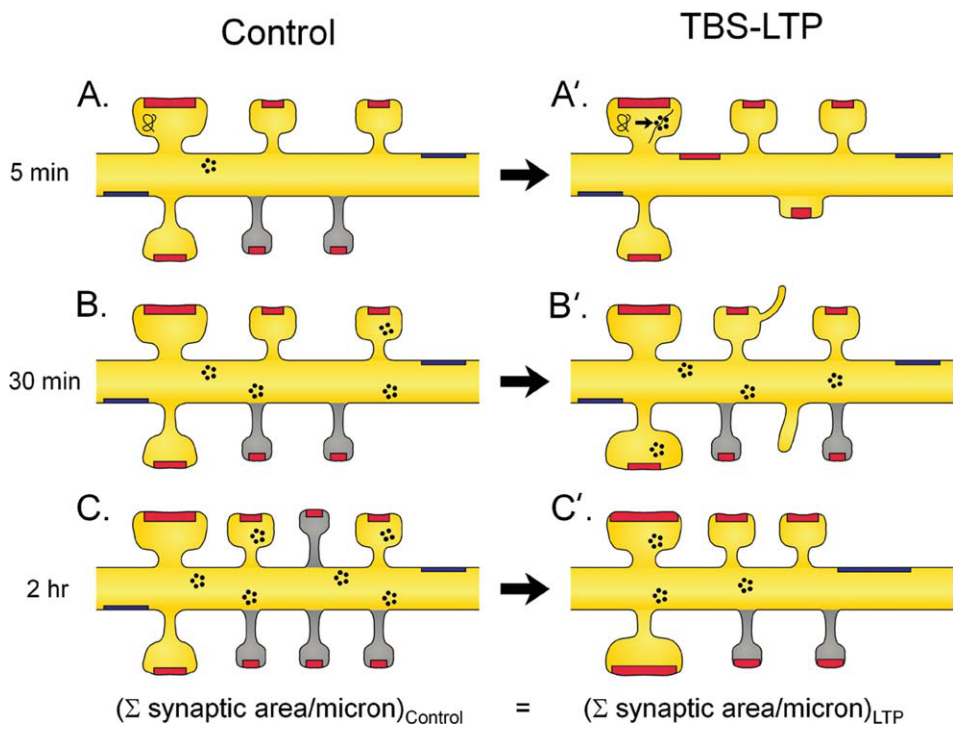


**FIGURE 11. Model of how induction of TBS-LTP results in rearrangement of excitatory and inhibitory synapses and a redistribution of polyribosomes. (A) Representation of a control dendrite (yellow) from the 5 min condition has excitatory (red) and inhibitory (blue) synapses and spines of all sizes, including small thin spines with diameters <0.45 microns (gray spines). The frequency of polyribosomes in these dendrites was relatively low (black circles). Some spines contain mRNAs that are masked (black line) and therefore not translating. (A′) At 5 min after TBS-LTP induction, asymmetric shaft synapses and stubby spines increased and polyribosomes were elevated in large spines with large synapses because mRNAs (black lines) were unmasked. (B) By 30 min, baseline stimulation in control dendrites had recruited polyribosomes while (B′) induction of TBS-LTP resulted in the emergence of nonsynaptic protrusions and the localization of polyribosomes to spines that had enlarged heads but had not yet enlarged their PSDs. (C) By 2 h, control dendrites demonstrated ongoing recovery of small thin spines, possibly in response to baseline stimulation whereas the (C′) induction of TBS-LTP either prevented the formation or promoted the elimination of those spines while enlarging the remaining PSDs. There was also a decrease in the frequency of inhibitory synapses that was accompanied by an enlargement in their size. In addition, polyribosomes decreased in number except in spines with large heads and enlarged PSDs by 2 h after induction of TBS-LTP. At each time point, the average summed synaptic area per unit length of dendrite for excitatory or inhibitory synapses remained stable across all conditions. [Color figure can be viewed in the online issue, which is available at wileyonlinelibrary.com.]**

new and labile spines continued to increase in number on control dendrites. Thus, the lower density of small spines 2 h after TBS-LTP induction could have resulted from selective elimination of nonpotentiated spines or the prevention of ongoing spinogenesis (similar to Bourne et al., 2007b). However, in contrast with our previous study, the average PSD area was significantly enlarged across all remaining typical spines, not just those containing polyribosomes (Bourne et al., 2007b). Small spines also turnover more frequently than large spines on both young and mature cortical dendrites (Holtmaat et al., 2005; Zuo et al., 2005a,b; Majewska et al., 2006). Small spines are selectively lost on basal CA1 dendrites following exposure to novel environments (Kitanishi et al., 2009a,b) and on cultured hippocampal dendrites outside the zone of synaptic activation (Engert and Bonhoeffer, 1999).

Spine loss might be triggered by several factors: secretion of an "elimination" signal from more effective synapses or surrounding glia (Lichtman and Colman, 2000; Stevens et al., 2007); insufficient activation to retain receptors (De Roo et al., 2008); a failure to recruit the mRNA or proteins needed to stabilize or enlarge the synapse (Frey and Morris, 1997; Martin and Kosik, 2002); or altered dendritic membrane properties (Losonczy and Magee, 2006; Losonczy et al., 2008). The spatial resolution of these potential interspine effects is not known, however, our findings show that counterbalancing strength vs. number of spine synapses can occur along mature dendritic segments less than 10 microns long.

Local protein synthesis is required to enlarge dendritic spines on developing neurons (Tanaka et al., 2008; Yang et al., 2008) and to sustain LTP (Steward and Schuman, 2001). The increase in polyribosomes in control dendrites over time suggests that local protein synthesis may also be required to promote synaptic recovery from slicing-induced trauma during the preparation of hippocampal slices (Fiala et al., 2003). The distribution of free polyribosomes following induction of TBS-LTP supports recent hypotheses that potentiated synapses might be "tagged" (Frey and Morris, 1997; Martin and Kosik, 2002; Ostroff et al., 2002; Bourne et al., 2007b), compete for

(Fonseca et al., 2004), replenish (Routtenberg and Rekart, 2005), and recycle proteins (Park et al., 2006) locally during the course of LTP. The transient elevation of polyribosomes in spines with large synapses at 5 min after TBS-LTP suggests that local mRNAs were immediately unmasked at existing strong synapses (Wu et al., 1998; Wells et al., 2000). Initial enlargement of spine heads has been associated with insertion of glutamate receptors (Grosshans et al., 2002; Matsuzaki et al., 2004; Kopec et al., 2006; Williams et al., 2007; Kerchner and Nicoll, 2008) which might be available via local recycling endosomes (Park et al., 2006). Free polyribosomes indicate synthesis of cytoplasmic proteins, hence candidate molecules might include PSD95 (Gray et al., 2006; Ehrlich et al., 2007), CAMKII (Otmakhov et al., 2004; Rose et al., 2009) or other PSD-associated molecules involved in stabilizing receptors (Kennedy, 2000). At 30 min after TBS-LTP the presence of polyribosomes in large spines, but lack of significant change in average PSD areas, suggests that mRNAs or polyribosomes were targeted to newly enlarged spines with PSDs that had not yet increased in size. Consistent with this hypothesis, we found at 2 h that the subset of spines containing polyribosomes had the largest PSDs, suggesting that LTP-specific synapse enlargement required and rapidly used local protein synthesis machinery in spines.

Replenishment of polyribosomes at enlarged synapses by 2 h after induction of LTP was accompanied by a loss of polyribosomes from dendritic shafts and neighboring smaller spines. A decrease in polyribosomes at the base of spines has also been observed in the mature dentate gyrus at various time points after LTP induced by the delivery of 17.5-ms trains of pulses at 400 Hz (Desmond and Levy, 1990). Thus, multiple trains of brief stimuli may be more effective in triggering and quickly translating proteins than the sustained 1-s pulse trains commonly used in tetanic stimulation. These observations indicate that translational machinery can be rapidly redistributed among spines along mature CA1 dendrites to an even greater extent following TBS-LTP than following tetanic-LTP in immature (Ostroff et al., 2002) or mature CA1 dendrites (Bourne et al., 2007b). TBS elevates calcium in dendrites from multiple sources including influx through NMDA receptors and voltage dependent calcium channels, as well as release from intracellular stores; whereas tetanic stimulation primarily elevates calcium through NMDA receptors (Raymond and Redman, 2002). TBS, but not tetanic stimulation, causes release of brain derived neurotrophic factor (BDNF), which enhances protein synthesis (Kang et al., 1997; Chen et al., 1999; Aakalu et al., 2001). Thus, the finding that TBS-LTP utilizes more polyribosomes than tetanic-LTP could be explained by the different signals triggered by the TBS and tetanic induction paradigms.

Symmetric shaft synapses also decreased in frequency and increased in size at 2 h after the induction of TBS-LTP. We confirmed that like mature CA1 dendrites in vivo (Megias et al., 2001), the symmetric synapses occurred on average only once every 5–10 μm along mature CA1 dendrites in hippocampal slices. Therefore, the symmetric synapses could modulate synaptic function among many dendritic spines before and after induction of TBS-LTP. These synapses are made by multiple types of interneurons that modulate or inhibit pyramidal cell excitability (Freund and Buzsaki, 1996; Gaiarsa et al., 2002; Klausberger and Somogyi, 2008). The axons of some interneurons, such as basket cells and bistratified cells, span *s. radiatum* and undergo LTD following high frequency stimulation, consequently reducing inhibition on neighboring CA1 pyramidal cells in adult hippocampus (Wang and Stelzer, 1996; McMahon and Kauer, 1997; Lu et al., 2000; Mendoza et al., 2006; Gibson et al., 2008). The loss of inhibitory synapses observed 2 h after TBS-LTP might account for this LTD and also reduce the LTP threshold of neighboring spines (Harvey and Svoboda, 2007). The increase in size of the remaining symmetric synapses could counterbalance unmitigated excitation that might ultimately become epileptogenic (Gaiarsa et al., 2002).

It is not known which synapses that were exposed to LTP-inducing stimuli were actually responsible for the expression of LTP. We maximized our ability to detect plasticity related structural changes by analyzing dendrites that were in the immediate vicinity of Schaffer collaterals that were stimulated by the bipolar electrodes. LTP is input specific at relatively long distances along axons (100's of microns), which we confirmed; however, pre- and postsynaptic organelles, molecules, and electrical signals spread amongst neighboring synapses for 10's of microns following induction of LTP at an individual synapse (Darcy et al., 2006; Harvey and Svoboda, 2007; Rose et al., 2009). Hence, whether individual synapses are visualized in the living state before and after induction of LTP or if a large number of dendrites and synapses in the path of TBS-LTP versus control stimulation are evaluated with ssTEM, one cannot be sure exactly which synapses mediate LTP. Others have used calcium-oxalate in an attempt to identify where synapse-specific calcium influx might have occurred following induction of LTP (Buchs and Muller, 1996); however, the electron dense calcium-oxalate precipitate shows high background and only those spines containing smooth endoplasmic reticulum accumulated enough precipitate in either the control or LTP conditions. Hence, this approach to identify specifically the potentiated synapses is biased because only about 10–15% of hippocampal dendritic spines contain SER (Spacek and Harris, 1997). Thus, it is not possible with available methods to define unequivocally which specific synapses were responsible for expressing LTP. Despite these caveats, it is reasonable to deduce that the enhanced response associated with LTP was mediated by the enlarged synapses that had captured polyribosomes. Furthermore, the ultrastructural changes reported here through ssTEM provide an expanded basis for understanding the timing and extent of ultrastructural mechanisms underlying LTP.

These results support the hypothesis that dendritic segments act as functional units (Rabinowitch and Segev, 2008). They show the first structural evidence that a loss in number is balanced by growth in size of the remaining, presumably potentiated, excitatory and inhibitory synapses by 2 h after induction of TBS-LTP. Global changes in synaptic activity that affect whole neurons show complementary effects in the mature

hippocampus, where excessive synaptic activation results in spine loss (Jiang et al., 1998) and silencing all synaptic activity results in excess spines (Kirov and Harris, 1999; Kirov et al., 2004a). These findings might also reflect a mechanism of homeostatic regulation that is occurring at a global level throughout the neuron (Nelson and Turrigiano, 2008) and also can be detected locally along individual dendrites.. Alternatively, the homeostatic balance of structural plasticity may be mediated locally for individual dendrites independent of the rest of the neuron (Rabinowitch and Segev, 2008). What might constitute a local regulatory mechanism operating in the less than 10-μm range? Synaptic resources including polyribosomes and intracellular organelles occur about once every 10 μm along mature dendrites (Spacek and Harris, 1997; Cooney et al., 2002; Park et al., 2006) and further study is needed to determine whether their capture serves to regulate which synapses are strengthened during LTP.

## Acknowledgments

The authors thank Elizabeth Perry and Robert Smith for technical assistance, Mr. Scott Schulz for artistic assistance, and Dr. John Fiala for developing the RECONSTRUCT™ software. They also thank Dan Johnston, Gina Turrigiano, Mitya Chklovskii, Dominique Muller, and Kimberly Raab-Graham for expert critiques of an earlier draft of this manuscript.

## REFERENCES

Aakalu G, Smith WB, Nguyen N, Jiang C, Schuman EM. 2001. Dynamic visualization of local protein synthesis in hippocampal neurons. Neuron 30:489–502.

Abraham WC, Huggett A. 1997. Induction and reversal of long-term potentiation by repeated high-frequency stimulation in rat hippocampal slices. Hippocampus 7:137–145.

Bliss TVP, Collingridge GL. 1993. A synaptic model of memory: Long-term potentiation in the hippocampus. Nature 361:31–39.

Bourne J, Harris KM. 2007. Do thin spines learn to be mushroom spines that remember? Curr Opin Neurobiol 17:381–386.

Bourne JN, Harris KM. 2008. Balancing structure and function at hippocampal dendritic spines. Annu Rev Neurosci 31:47–67.

Bourne JN, Kirov SA, Sorra KE, Harris KM. 2007a. Warmer preparation of hippocampal slices prevents synapse proliferation that might obscure LTP-related structural plasticity. Neuropharmacology 52:55–59.

Bourne JN, Sorra KE, Hurlburt J, Harris KM. 2007b. Polyribosomes are increased in spines of CA1 dendrites 2 h after the induction of LTP in mature rat hippocampal slices. Hippocampus 17:1–4.

Bracci E, Vreugdenhil M, Hack SP, Jefferys JG. 1999. On the synchronizing mechanisms of tetanically induced hippocampal oscillations. J Neurosci 19:8104–8113.

Buchs PA, Muller D. 1996. Induction of long-term potentiation is associated with major ultrastructural changes of activated synapses. Proc Natl Acad Sci USA 93:8040–8045.

Buzsaki G. 2002. Theta oscillations in the hippocampus. Neuron 33:325–340.

Buzsaki G, Haas HL, Anderson EG. 1987. Long-term potentiation induced by physiologically relevant stimulus patterns. Brain Res 435:331–333.

Chang FL, Greenough WT. 1984. Transient and enduring morphological correlates of synaptic activity and efficacy change in the rat hippocampal slice. Brain Res 309:35–46.

Chen G, Kolbeck R, Barde YA, Bonhoeffer T, Kossel A. 1999. Relative contribution of endogenous neurotrophins in hippocampal long-term potentiation. J Neurosci 19:7983–7990.

Colonnier M. 1968. Synaptic patterns on different cell types in the different laminae of the cat visual cortex. An electron microscope study. Brain Res 9:268–287.

Cooney JR, Hurlburt JL, Selig DK, Harris KM, Fiala JC. 2002. Endosomal compartments serve multiple hippocampal dendritic spines from a widespread rather than a local store of recycling membrane. J Neurosci 22:2215–2224.

Corera AT, Doucet G, Fon EA. 2009. Long-term potentiation in isolated dendritic spines. PLoS One 4:e6021.

Dailey ME, Smith SJ. 1996. The dynamics of dendritic structure in developing hippocampal slices. J Neurosci 16:2983–2994.

Darcy KJ, Staras K, Collinson LM, Goda Y. 2006. Constitutive sharing of recycling synaptic vesicles between presynaptic boutons. Nat Neurosci 9:315–321.

De Roo M, Klauser P, Muller D. 2008. LTP promotes a selective long-term stabilization and clustering of dendritic spines. PLoS Biol 6:e219.

Desmond NL, Levy WB. 1983. Synaptic correlates of associative potentiation/depression: An ultrastructural study in the hippocampus. Brain Res 265:21–30.

Desmond NL, Levy WB. 1986a. Changes in the numerical density of synaptic contacts with long-term potentiation in the hippocampal dentate gyrus. J Comp Neurol 253:466–475.

Desmond NL, Levy WB. 1986b. Changes in the postsynaptic density with long-term potentiation in the dentate gyrus. J Comp Neurol 253:476–482.

Desmond NL, Levy WB. 1990. Morphological correlates of long-term potentiation imply the modification of existing synapses, not synaptogenesis, in the hippocampal dentate gyrus. Synapse 5:139–143.

Ehrlich I, Klein M, Rumpel S, Malinow R. 2007. PSD-95 is required for activity-driven synapse stabilization. Proc Natl Acad Sci USA 104:4176–4181.

Engert F, Bonhoeffer T. 1999. Dendritic spine changes associated with hippocampal long-term synaptic plasticity. Nature 399:66–70.

Enoki R, Hu YL, Hamilton D, Fine A. 2009. Expression of long-term plasticity at individual synapses in hippocampus is graded, bidirectional, and mainly presynaptic: Optical quantal analysis. Neuron 62:242–253.

Fiala JC. 2005. Reconstruct: A free editor for serial section microscopy. J Microsc 218:52–61.

Fiala JC, Harris KM. 2001a. Cylindrical diameters method for calibrating section thickness in serial electron microscopy. J Microsc 202:468–472.

Fiala JC, Harris KM. 2001b. Extending unbiased stereology of brain ultrastructure to three-dimensional volumes. J Am Med Inform Assoc 8:1–16.

Fiala JC, Feinberg M, Popov V, Harris KM. 1998. Synaptogenesis via dendritic filopodia in developing hippocampal area CA1. J Neurosci 18:8900–8911.

Fiala JC, Kirov SA, Feinberg MD, Petrak LJ, George P, Goddard CA, Harris KM. 2003. Timing of neuronal and glial ultrastructure disruption during brain slice preparation and recovery in vitro. J Comp Neurol 465:90–103.

Fifkova E, Anderson CL. 1981. Stimulation-induced changes in dimensions of stalks of dendritic spines in the dentate molecular layer. Exp Neurol 74:621–627.

Fifkova E, Van Harreveld A. 1977. Long-lasting morphological changes in dendritic spines of dentate granular cells following stimulation of the entorhinal area. J Neurocytol 6:211–230.

Fonseca R, Nagerl UV, Morris RG, Bonhoeffer T. 2004. Competing for memory: Hippocampal LTP under regimes of reduced protein synthesis. Neuron 44:1011–1020.

Freund TF, Buzsaki G. 1996. Interneurons of the hippocampus. Hippocampus 6:347–470.
Frey U, Morris RG. 1997. Synaptic tagging and long-term potentiation. Nature 385:533–536.
Gaiarsa JL, Caillard O, Ben-Ari Y. 2002. Long-term plasticity at GABAergic and glycinergic synapses: Mechanisms and functional significance. Trends Neurosci 25:564–570.
Geinisman Y, Toledo-Morrell L, Morrell F. 1991. Induction of long-term potentiation is associated with an increase in the number of axospinous synapses with segmented postsynaptic densities. Brain Res 566:77–88.
Geinisman Y, de Toledo-Morrell L, Morrell F, Heller RE, Rossi M, Parshall RF. 1993. Structural synaptic correlate of long-term potentiation: Formation of axospinous synapses with multiple, completely partitioned transmission zones. Hippocampus 3:435–445.
Gibson HE, Edwards JG, Page RS, Van Hook MJ, Kauer JA. 2008. TRPV1 channels mediate long-term depression at synapses on hippocampal interneurons. Neuron 57:746–759.
Govindarajan A, Kelleher RJ, Tonegawa S. 2006. A clustered plasticity model of long-term memory engrams. Nat Rev Neurosci 7:575–583.
Gray NW, Weimer RM, Bureau I, Svoboda K. 2006. Rapid redistribution of synaptic PSD-95 in the neocortex in vivo. PLoS Biol 4:e370.
Grosshans DR, Clayton DA, Coultrap SJ, Browning MD. 2002. LTP leads to rapid surface expression of NMDA but not AMPA receptors in adult rat CA1. Nat Neurosci 5:27–33.
Harris KM. 1999. Structure, development, and plasticity of dendritic spines. Curr Opin Neurobiol 9:343–348.
Harris KM, Marshall PE, Landis DM. 1985. Ultrastructural study of cholecystokinin-immunoreactive cells and processes in area CA1 of the rat hippocampus. J Comp Neurol 233:147–158.
Harris KM, Jensen FE, Tsao B. 1992. Three-dimensional structure of dendritic spines and synapses in rat hippocampus (CA1) at postnatal day 15 and adult ages: Implications for the maturation of synaptic physiology and long-term potentiation. J Neurosci 12:2685–2705.
Harris KM, Perry E, Bourne J, Feinberg M, Ostroff L, Hurlburt J. 2006. Uniform serial sectioning for transmission electron microscopy. J Neurosci 26:12101–12103.
Harvey CD, Svoboda K. 2007. Locally dynamic synaptic learning rules in pyramidal neuron dendrites. Nature 450:1195–1200.
Harvey CD, Yasuda R, Zhong H, Svoboda K. 2008. The spread of Ras activity triggered by activation of a single dendritic spine. Science 321:136–140.
Holtmaat AJ, Trachtenberg JT, Wilbrecht L, Shepherd GM, Zhang X, Knott GW, Svoboda K. 2005. Transient and persistent dendritic spines in the neocortex in vivo. Neuron 45:279–291.
Hosokawa T, Rusakov DA, Bliss TV, Fine A. 1995. Repeated confocal imaging of individual dendritic spines in the living hippocampal slice: Evidence for changes in length and orientation associated with chemically induced LTP. J Neurosci 15:5560–5573.
Hyman JM, Wyble BP, Goyal V, Rossi CA, Hasselmo ME. 2003. Stimulation in hippocampal region CA1 in behaving rats yields long-term potentiation when delivered to the peak of theta and long-term depression when delivered to the trough. J Neurosci 23:11725–11731.
Jensen FE, Harris KM. 1989. Preservation of neuronal ultrastructure in hippocampal slices using rapid microwave-enhanced fixation. J Neurosci Methods 29:217–230.
Jiang M, Lee CL, Smith KL, Swann JW. 1998. Spine loss and other persistent alterations of hippocampal pyramidal cell dendrites in a model of early-onset epilepsy. J Neurosci 18:8356–8368.
Kang H, Welcher AA, Shelton D, Schuman EM. 1997. Neurotrophins and time: Different roles for TrkB signaling in hippocampal long-term potentiation. Neuron 19:653–664.
Kennedy MB. 2000. Signal-processing machines at the postsynaptic density. Science 290:750–754.
Kerchner GA, Nicoll RA. 2008. Silent synapses and the emergence of a postsynaptic mechanism for LTP. Nat Rev Neurosci 9:813–825.
Kirov SA, Harris KM. 1999. Dendrites are more spiny on mature hippocampal neurons when synapses are inactivated. Nat Neurosci 2:878–883.
Kirov SA, Sorra KE, Harris KM. 1999. Slices have more synapses than perfusion-fixed hippocampus from both young and mature rats. J Neurosci 19:2876–2886.
Kirov SA, Goddard CA, Harris KM. 2004a. Age-dependence in the homeostatic upregulation of hippocampal dendritic spine number during blocked synaptic transmission. Neuropharmacology 47:640–648.
Kirov SA, Petrak LJ, Fiala JC, Harris KM. 2004b. Dendritic spines disappear with chilling but proliferate excessively upon rewarming of mature hippocampus. Neurosci 127:69–80.
Kitanishi T, Ikegaya Y, Matsuki N. 2009a. Behaviorally evoked transient reorganization of hippocampal spines. Eur J Neurosci 30:560–566.
Kitanishi T, Ikegaya Y, Matsuki N, Yamada MK. 2009b. Experience-dependent, rapid structural changes in hippocampal pyramidal cell spines. Cereb Cortex 19:2572–2578.
Klausberger T, Somogyi P. 2008. Neuronal diversity and temporal dynamics: The unity of hippocampal circuit operations. Science 321:53–57.
Knott GW, Quairiaux C, Genoud C, Welker E. 2002. Formation of dendritic spines with GABAergic synapses induced by whisker stimulation in adult mice. Neuron 34:265–273.
Kopec CD, Li B, Wei W, Boehm J, Malinow R. 2006. Glutamate receptor exocytosis and spine enlargement during chemically induced long-term potentiation. J Neurosci 26:2000–2009.
Kopec CD, Real E, Kessels HW, Malinow R. 2007. GluR1 links structural and functional plasticity at excitatory synapses. J Neurosci 27:13706–13718.
Lang C, Barco A, Zablow L, Kandel ER, Siegelbaum SA, Zakharenko SS. 2004. Transient expansion of synaptically connected dendritic spines upon induction of hippocampal long-term potentiation. Proc Natl Acad Sci USA 101:16665–16670.
Larson J, Wong D, Lynch G. 1986. Patterned stimulation at the theta frequency is optimal for the induction of hippocampal long-term potentiation. Brain Res 368:347–350.
Lee KS, Schottler F, Oliver M, Lynch G. 1980. Brief bursts of high-frequency stimulation produce two types of structural change in rat hippocampus. J. Neurophysiol. 44:247–258.
Lee SJ, Escobedo-Lozoya Y, Szatmari EM, Yasuda R. 2009. Activation of CaMKII in single dendritic spines during long-term potentiation. Nature 458:299–304.
Lichtman JW, Colman H. 2000. Synapse elimination and indelible memory. Neuron 25:269–278.
Lisman J, Raghavachari S. 2006. A unified model of the presynaptic and postsynaptic changes during LTP at CA1 synapses. Sci STKE 2006:re11.
Losonczy A, Magee JC. 2006. Integrative properties of radial oblique dendrites in hippocampal CA1 pyramidal neurons. Neuron 50:291–307.
Losonczy A, Makara JK, Magee JC. 2008. Compartmentalized dendritic plasticity and input feature storage in neurons. Nature 452:436–441.
Lu YM, Mansuy IM, Kandel ER, Roder J. 2000. Calcineurin-mediated LTD of GABAergic inhibition underlies the increased excitability of CA1 neurons associated with LTP. Neuron 26:197–205.
Magee JC, Johnston D. 1997. A synaptically controlled, associative signal for Hebbian plasticity in hippocampal neurons. Science 275:209–213.
Magee JC, Johnston D. 2005. Plasticity of dendritic function. Curr Opin Neurobiol 15:334–342.

Majewska AK, Newton JR, Sur M. 2006. Remodeling of synaptic structure in sensory cortical areas in vivo. J Neurosci 26:3021–3029.

Makara JK, Losonczy A, Wen Q, Magee JC. 2009. Experience-dependent compartmentalized dendritic plasticity in rat hippocampal CA1 pyramidal neurons. Nat Neurosci 12:1485–1487.

Maletic-Savatic M, Malinow R, Svoboda K. 1999. Rapid dendritic morphogenesis in CA1 hippocampal dendrites induced by synaptic activity. Science 283:1923–1927.

Martin KC, Kosik KS. 2002. Synaptic tagging—Who's it? Nat Rev Neurosci 3:813–820.

Matsuzaki M, Honkura N, Ellis-Davies GC, Kasai H. 2004. Structural basis of long-term potentiation in single dendritic spines. Nature 429:761–766.

McMahon LL, Kauer JA. 1997. Hippocampal interneurons express a novel form of synaptic plasticity. Neuron 18:295–305.

Medalia O, Weber I, Frangakis AS, Nicastro D, Gerisch G, Baumeister W. 2002. Macromolecular architecture in eukaryotic cells visualized by cryoelectron tomography. Science 298:1209–1213.

Megias M, Emri Z, Freund TF, Gulyas AI. 2001. Total number and distribution of inhibitory and excitatory synapses on hippocampal CA1 pyramidal cells. Neurosci 102:527–540.

Mendoza E, Galarraga E, Tapia D, Laville A, Hernandez-Echeagaray E, Bargas J. 2006. Differential induction of long term synaptic plasticity in inhibitory synapses of the hippocampus. Synapse 60:533–542.

Morgan SL, Teyler TJ. 2001. Electrical stimuli patterned after the theta-rhythm induce multiple forms of LTP. J Neurophysiol 86:1289–1296.

Nagerl UV, Eberhorn N, Cambridge SB, Bonhoeffer T. 2004. Bidirectional activity-dependent morphological plasticity in hippocampal neurons. Neuron 44:759–767.

Nagerl UV, Kostinger G, Anderson JC, Martin KA, Bonhoeffer T. 2007. Protracted synaptogenesis after activity-dependent spinogenesis in hippocampal neurons. J Neurosci 27:8149–8156.

Nelson SB, Turrigiano GG. 2008. Strength through diversity. Neuron 60:477–482.

Nguyen PV, Kandel ER. 1997. Brief theta-burst stimulation induces a transcription-dependent late phase of LTP requiring cAMP in area CA1 of the mouse hippocampus. Learn Mem 4:230–243.

Ostroff LE, Fiala JC, Allwardt B, Harris KM. 2002. Polyribosomes redistribute from dendritic shafts into spines with enlarged synapses during LTP in developing rat hippocampal slices. Neuron 35:535–545.

Otmakhov N, Tao-Cheng JH, Carpenter S, Asrican B, Dosemeci A, Reese TS, Lisman J. 2004. Persistent accumulation of calcium/calmodulin-dependent protein kinase II in dendritic spines after induction of NMDA receptor-dependent chemical long-term potentiation. J Neurosci 24:9324–9331.

Ouyang Y, Kantor D, Harris KM, Schuman EM, Kennedy MB. 1997. Visualization of the distribution of autophosphorylated calcium/calmodulin-dependent protein kinase II after tetanic stimulation in the CA1 area of the hippocampus. J Neurosci 17:5416–5427.

Park M, Salgado JM, Ostroff L, Helton TD, Robinson CG, Harris KM, Ehlers MD. 2006. Plasticity-induced growth of dendritic spines by exocytic trafficking from recycling endosomes. Neuron 52:817–830.

Peters A, Palay SL, Webster HD. 1991. The fine structure of the nervous system: The neurons and supporting cells. Philadelphia: W.B. Saunders.1 p.

Petrak LJ, Harris KM, Kirov SA. 2005. Synaptogenesis on mature hippocampal dendrites occurs via filopodia and immature spines during blocked synaptic transmission. J Comp Neurol 484:183–190.

Poirazi P, Mel BW. 2001. Impact of active dendrites and structural plasticity on the memory capacity of neural tissue. Neuron 29:779–796.

Polsky A, Mel BW, Schiller J. 2004. Computational subunits in thin dendrites of pyramidal cells. Nat Neurosci 7:621–627.

Popov VI, Davies HA, Rogachevsky VV, Patrushev IV, Errington ML, Gabbott PL, Bliss TV, Stewart MG. 2004. Remodelling of synaptic morphology but unchanged synaptic density during late phase long-term potentiation (LTP): A serial section electron micrograph study in the dentate gyrus in the anaesthetised rat. Neuroscience 128:251–262.

Rabinowitch I, Segev I. 2008. Two opposing plasticity mechanisms pulling a single synapse. Trends Neurosci 31:377–383.

Raymond CR. 2008. Different requirements for action potentials in the induction of different forms of long-term potentiation. J Physiol 586:1859–1865.

Raymond CR, Redman SJ. 2002. Different calcium sources are narrowly tuned to the induction of different forms of LTP. J Neurophysiol 88:249–255.

Raymond CR, Redman SJ. 2006. Spatial segregation of neuronal calcium signals encodes different forms of LTP in rat hippocampus. J Physiol 570:97–111.

Richards DA, Mateos JM, Hugel S, De P,V, Caroni P, Gahwiler BH, McKinney RA. 2005. Glutamate induces the rapid formation of spine head protrusions in hippocampal slice cultures. Proc Natl Acad Sci USA 102:6166–6171.

Robinson CV, Sali A, Baumeister W. 2007. The molecular sociology of the cell. Nature 450:973–982.

Rose J, Jin SX, Craig AM. 2009. Heterosynaptic molecular dynamics: Locally induced propagating synaptic accumulation of CaM kinase II. Neuron 61:351–358.

Routtenberg A, Rekart JL. 2005. Post-translational protein modification as the substrate for long-lasting memory. Trends Neurosci 28:12–19.

Sorra KE, Harris KM. 1998. Stability in synapse number and size at 2 hr after long-term potentiation in hippocampal area CA1. J Neurosci 18:658–671.

Spacek J, Harris KM. 1997. Three-dimensional organization of smooth endoplasmic reticulum in hippocampal CA1 dendrites and dendritic spines of the immature and mature rat. J Neurosci 17:190–203.

Staubli U, Lynch G. 1987. Stable hippocampal long-term potentiation elicited by "theta" pattern stimulation. Brain Res 435:227–234.

Stevens B, Allen NJ, Vazquez LE, Howell GR, Christopherson KS, Nouri N, Micheva KD, Mehalow AK, Huberman AD, Stafford B, Sher A, Litke AM, Lambris JD, Smith SJ, John SW, Barres BA. 2007. The classical complement cascade mediates CNS synapse elimination. Cell 131:1164–1178.

Steward O, Schuman EM. 2001. Protein synthesis at synaptic sites on dendrites. Annu Rev Neurosci 24:299–325.

Stewart MG, Medvedev NI, Popov VI, Schoepfer R, Davies HA, Murphy K, Dallerac GM, Kraev IV, Rodriguez JJ. 2005. Chemically induced long-term potentiation increases the number of perforated and complex postsynaptic densities but does not alter dendritic spine volume in CA1 of adult mouse hippocampal slices. Eur J Neurosci 21:3368–3378.

Sutton MA, Schuman EM. 2005. Local translational control in dendrites and its role in long-term synaptic plasticity. J Neurobiol 64:116–131.

Tanaka J, Horiike Y, Matsuzaki M, Miyazaki T, Ellis-Davies GC, Kasai H. 2008. Protein synthesis and neurotrophin-dependent structural plasticity of single dendritic spines. Science 319:1683–1687.

Tao-Cheng JH, Gallant PE, Brightman MW, Dosemeci A, Reese TS. 2007. Structural changes at synapses after delayed perfusion fixation in different regions of the mouse brain. J Comp Neurol 501:731–740.

Trommald M, Vaaland JL, Blackstad TW, Andersen P. 1990. Dendritic spine changes in rat dentate granule cells associated with long-term potentiation. In: Guidotti A, Costa E, editors. Neurotoxicity of Excitatory Amino Acids. New York: Raven Press. pp 163–174.

Trommald M, Hulleberg G, Andersen P. 1996. Long-term potentiation is associated with new excitatory spine synapses on rat dentate granule cells. Learn Mem 3:218–228.

Tsuriel S, Geva R, Zamorano P, Dresbach T, Boeckers T, Gundelfinger ED, Garner CC, Ziv NE. 2006. Local sharing as a predominant determinant of synaptic matrix molecular dynamics. PLoS Biol 4:e271.

Vreugdenhil M, Bracci E, Jefferys JG. 2005. Layer-specific pyramidal cell oscillations evoked by tetanic stimulation in the rat hippocampal area CA1 in vitro and in vivo. J Physiol 562:149–164.

Wang JH, Stelzer A. 1996. Shared calcium signaling pathways in the induction of long-term potentiation and synaptic disinhibition in CA1 pyramidal cell dendrites. J Neurophysiol 75:1687–1702.

Wells DG, Richter JD, Fallon JR. 2000. Molecular mechanisms for activity-regulated protein synthesis in the synapto-dendritic compartment. Curr Opin Neurobiol 10:132–137.

Whittington MA, Stanford IM, Colling SB, Jefferys JG, Traub RD. 1997. Spatiotemporal patterns of gamma frequency oscillations tetanically induced in the rat hippocampal slice. J Physiol 502 (Part 3):591–607.

Williams JM, Guevremont D, Mason-Parker SE, Luxmanan C, Tate WP, Abraham WC. 2007. Differential trafficking of AMPA and NMDA receptors during long-term potentiation in awake adult animals. J Neurosci 27:14171–14178.

Wu L, Wells D, Tay J, Mendis D, Abbott MA, Barnitt A, Quinlan E, Heynen A, Fallon JR, Richter JD. 1998. CPEB-mediated cytoplasmic polyadenylation and the regulation of experience-dependent translation of alpha-CaMKII mRNA at synapses. Neuron 21:1129–1139.

Yang Y, Wang XB, Frerking M, Zhou Q. 2008. Spine expansion and stabilization associated with long-term potentiation. J Neurosci 28:5740–5751.

Yankova M, Hart SA, Woolley CS. 2001. Estrogen increases synaptic connectivity between single presynaptic inputs and multiple postsynaptic CA1 pyramidal cells: A serial electronmicroscopic study. Proc Natl Acad Sci USA 98:3525–3530.

Yuste R, Bonhoeffer T. 2001. Morphological changes in dendritic spines associated with long-term synaptic plasticity. Annu Rev Neurosci 24:1071–1089.

Yuste R, Bonhoeffer T. 2004. Genesis of dendritic spines: Insights from ultrastructural and imaging studies. Nat Rev Neurosci 5:24–34.

Zakharenko SS, Zablow L, Siegelbaum SA. 2001. Visualization of changes in presynaptic function during long-term synaptic plasticity. Nat Neurosci 4:711–717.

Zhong H, Sia GM, Sato TR, Gray NW, Mao T, Khuchua Z, Huganir RL, Svoboda K. 2009. Subcellular dynamics of type II PKA in neurons. Neuron 62:363–374.

Zuo Y, Lin A, Chang P, Gan WB. 2005a. Development of long-term dendritic spine stability in diverse regions of cerebral cortex. Neuron 46:181–189.

Zuo Y, Yang G, Kwon E, Gan WB. 2005b. Long-term sensory deprivation prevents dendritic spine loss in primary somatosensory cortex. Nature 436:261–265.

| Filename | Format | Size | Description |
|---|---|---|---|
| HIPO_20768_sm_suppfig1.tif | | 67K | Supporting Figure 1: All of the reconstructed dendrites (black diamonds) were of a caliber across which spine density was not correlated with dendrite diameter (n=63 dendrites; r=0.24, n.s.). |
| HIPO_20768_sm_suppfig2.tif | | 11028K | Supporting Figure 2: Images across serial sections further define characteristics. (A-D) Serial section images through most of the macular PSD (black arrow) of the thin spine shown in Figure 5A, and through most of a symmetric synapse shown in figure 8A (white arrow). (E-H) Serial section images through some of the mushroom spine shown in Figure 5B illustrating a small perforation in the PSD (black arrow). (I-L) Serial sections through the branch point (thick arrows) of the spine shown in Figure 5C. Two thin spine heads (thin arrows) that form macular synapses on two different presynaptic axons (ax1 and ax2). Scale bar = 0.5 µm. |
| HIPO_20768_sm_suppfig3.tif | | 133K | Supporting Figure 3: PSD area of transitional synapses was similar across time. The distribution of PSD areas across asymmetric shaft synapses, stubby spines and multisynaptic spines was plotted for 5 min, 30 min, and 2 hr for control (light gray diamonds) and TBS-LTP (dark gray diamonds) dendrites. Red horizontal lines represent the averages (n=number of synapses). |
| HIPO_20768_sm_suppfig4.tif | | 8227K | Supporting Figure 4: Identification of polyribosomes by viewing through adjacent serial thin sections of (A-D) a dendritic shaft and (E-H) a dendritic spine. We used RECONSTRUCTTM interactively to enhance the contrast for unambiguous identification of polyribosomes relative to Supplemental Figure 2 where lower contrast was needed to distinguish the synaptic cleft from the PSD. Two polyribosomes were identified in this segment of the dendritic shaft (Black arrows on sections B and C). One polyribosome was identified in the head of the dendritic spine (Black arrow on section F). White arrows indicate the location of PR on adjacent sections where no structures are present that resemble PR, indicating their existence in only 1 or 2 sections, consistent with the number of individual ribosomes in each cluster. The line in H indicates the widest extent of this spine head, where the diameter was measured. Scale bar = 0.5 µm. |
| HIPO_20768_sm_suppfig5.tif | | 158K | Supporting Figure 5: Ongoing spine and synapse recovery in dendrites that received control stimulation only was associated with an increase in local protein synthesis. (A) Small thin spines < 0.45 microns in diameter were significantly increased along control dendrites after 2 hr of control stimulation (*p<0.05). (B) Polyribosomes were elevated by 30 min in the shaft and in the head and neck of dendritic spines in control dendrites (**p<0.01) and increased in frequency at the base of dendritic spines after 2 hr of control stimulation (*p<0.05). |
| HIPO_20768_sm_supptable1.doc | | 28K | Supporting Table 1: A summary of all the animals, dendrites and synapses that were included in the statistical analyses. |

Bourne and Harris Supplemental Figure 1

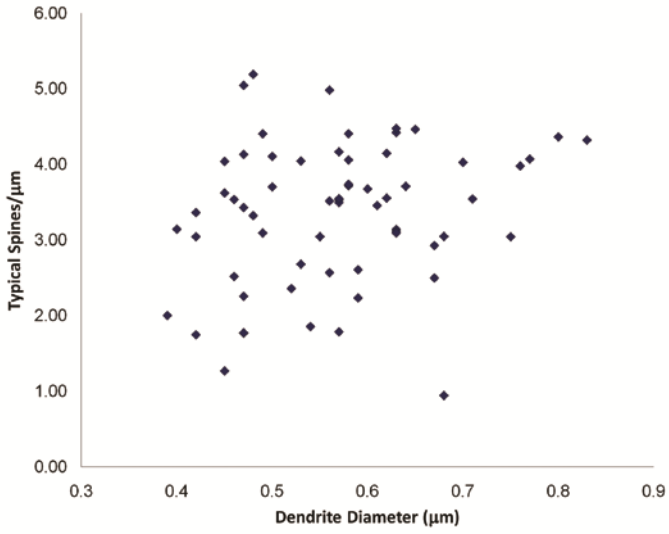

Bourne and Harris Supplemental Figure 2

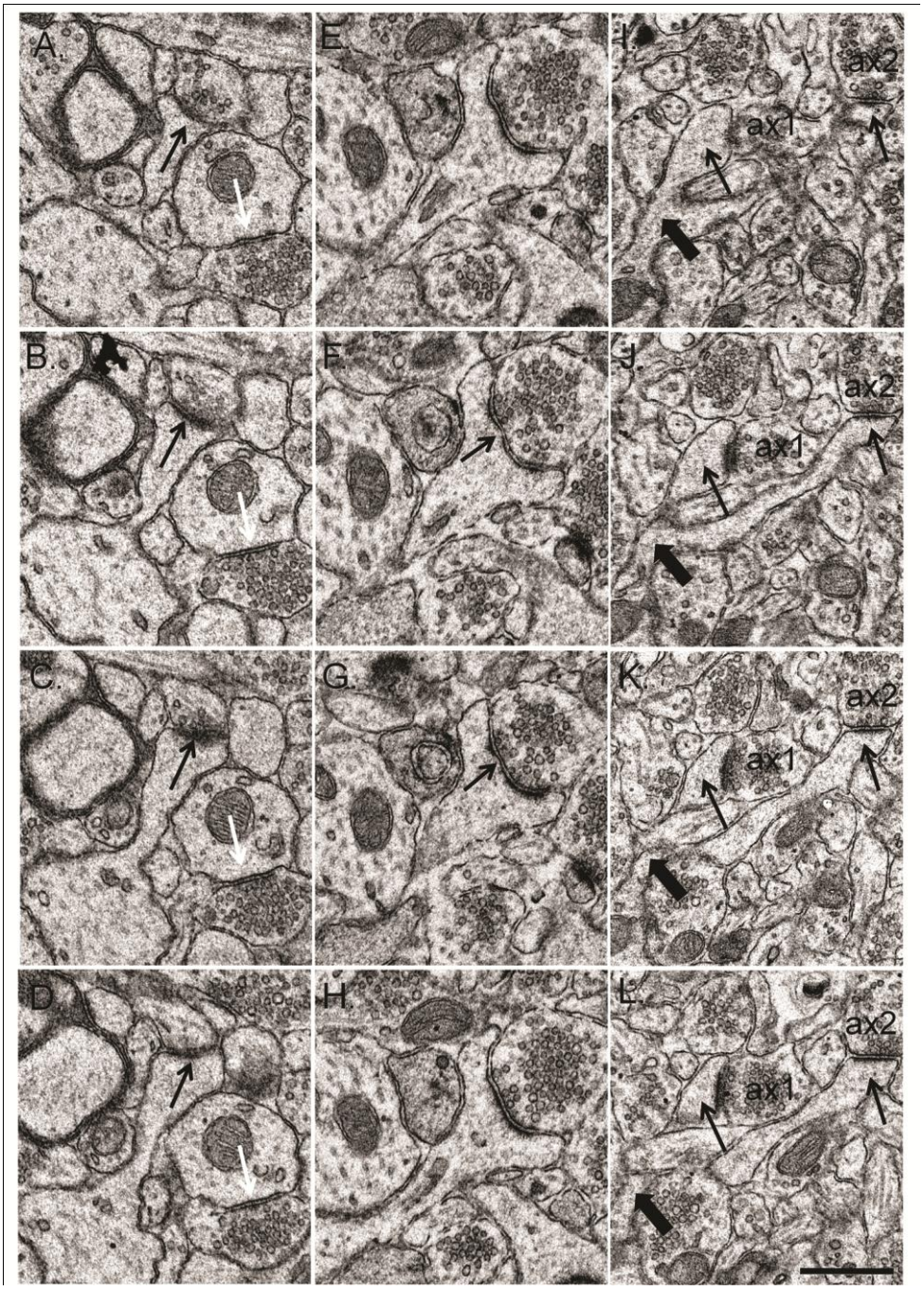

Bourne and Harris Supplemental Figure 3

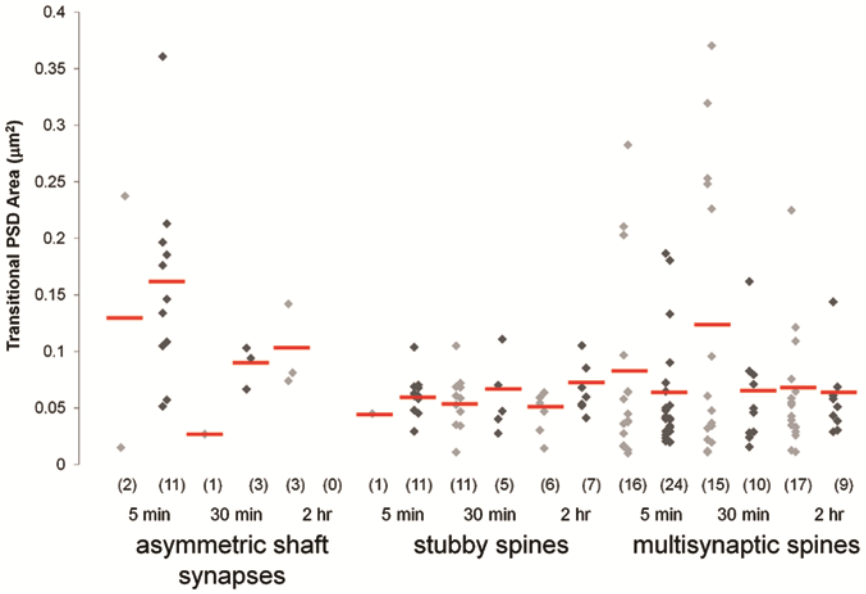

Bourne and Harris Supplemental Figure 4

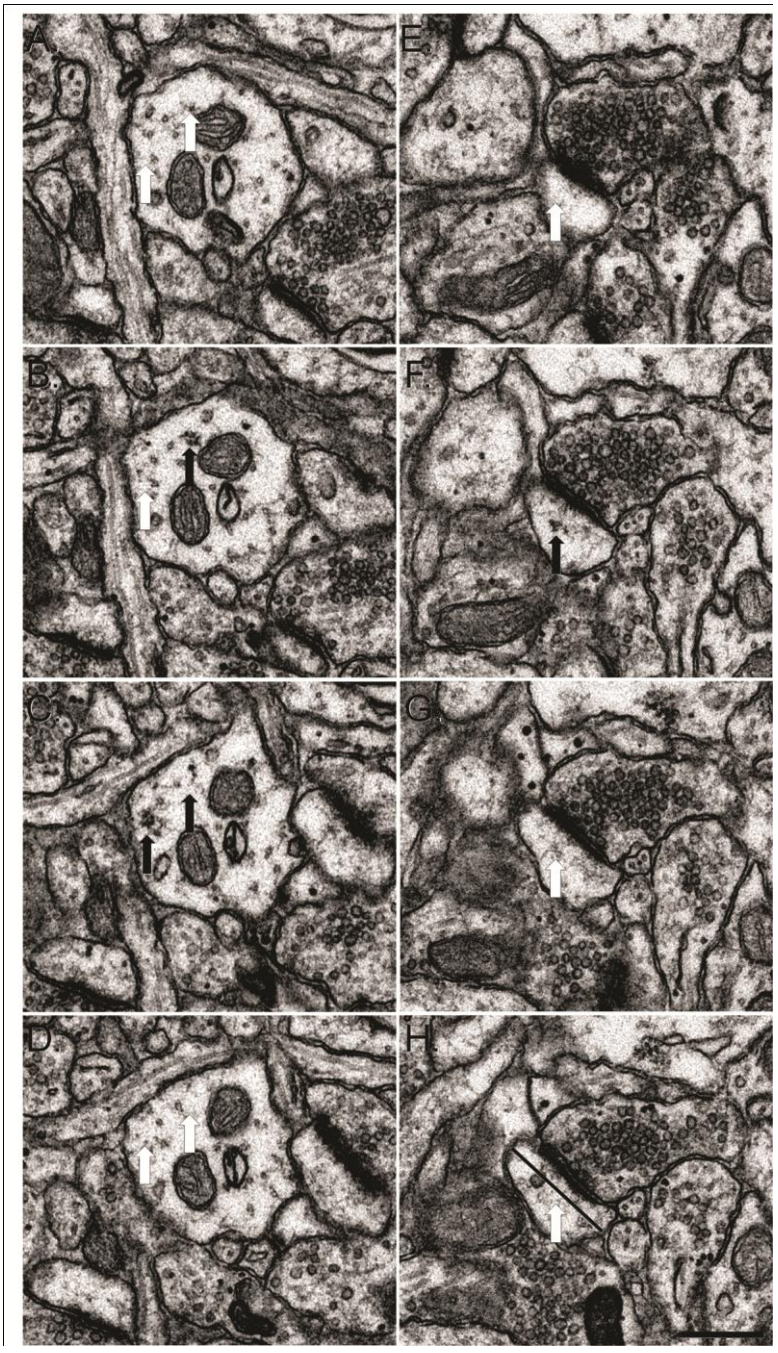

Bourne and Harris Supplemental Figure 5

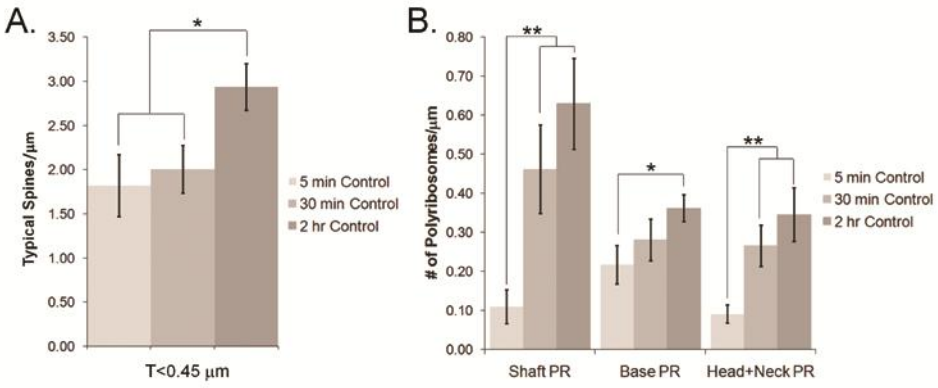

Supplemental Table 1: Summary of Experimental N's

| | Animals | Dendrites | | Asymmetric Synapses | | Symmetric Synapses | |
|---|---|---|---|---|---|---|---|
| | | Control | TBS-LTP | Control | TBS-LTP | Control | TBS - LTP |
| **5 min** | 3 | 10 | 10 | 311 | 272 | 22 | 18 |
| **30 min** | 3 | 12 | 13 | 308 | 364 | 14 | 17 |
| **2 hr** | 2 | 9 | 9 | 270 | 366 | 15 | 10 |